Analysis of meteorological parameters triggering rainfall induced landslide: a review of 70 years in Valtellina

Andrea Abbate[1], Monica Papini[1], Laura Longoni[1]

[1] Department of Civil Engineering (DICA), Politecnico di Milano, Milano 20133, Italy

Correspondence to: Laura Longoni (laura.longoni@polimi.it)

Abstract. This paper presents an extended reanalysis of the rainfall-induced ~~hydrogeological~~geo-hydrological events that occurred in the last 70 years in the alpine area of the Lombardy region, Italy. The work is focused on the description of the major meteorological triggering factors that have caused diffuse episodes of shallow landslide and debris flow. The aim of this reanalysis was to try to evaluate their magnitude quantitatively.

The triggering factors were studied following two approaches. The first one started from the conventional analysis of the rainfall intensity (I) and duration (D) considering local rain-gauge data and applying the I-D threshold methodology~~,~~ integrated with an estimation of the events' return period. We then extended this analysis and proposed a new index for the magnitude assessment (MI) based on frequency-magnitude theory. The MI index was defined considering both the return period and the spatial extension of each rainfall episode.

The second approach is based on a regional scale analysis of meteorological trigger. In particular, the strength of the extratropical cyclone structure (EC) associated with the precipitation events was assessed through the Sea Level Pressure Tendency (SLPT) meteorological index. The former has been estimated from the Norwegian Cyclone Model (NCM) theory.

Both indexes have shown an agreement in ranking the event's magnitude ($R^2 = 0.88$) giving a similar interpretation of the severity that was found also in accordance with the information reported in historical databases.

This back analysis of 70 years in Valtellina identifies the MI and the SLPT as good magnitude indicators of the event, confirming that a strong cause-effect relationship exists among the EC intensity and the local rainfalls recorded~~effects~~ on the ground. In respect to the conventional I-D threshold methodology, which is limited to a binary estimate of likelihood of landslide occurrence, the evaluation of the MI and the SLPT indexes allow~~permit~~ to quantify the magnitude of a rainfall episode capable to generate severe ~~hydrogeological~~geo-hydrological hazards.

1 Introduction

In the context of ~~hydrogeological~~geo-hydrological risk prevention, urban planners and infrastructure engineers still need instruments for carrying out trigger's analysis (Ozturk et al., 2015; Papini et al., 2017; Piciullo et al., 2017). This is crucial in

ha formattato: Inglese (Stati Uniti)

Codice campo modificato

ha formattato: Inglese (Stati Uniti)

ha formattato: Inglese (Stati Uniti)

that places where the natural landscape has been dramatically modified by uncontrolled urbanization ~~in order~~ to avoid human injures and material damages (Albano et al., 2017b; Bronstert et al., 2018). Italy is a country historically affected by a diffuse ~~hydrogeological~~geo-hydrological fragility (Albano et al., 2017a; Ballio et al., 2010; Caine, 1980; Gao et al., 2018; Longoni et al., 2016) ~~Longoni et al., 2016)~~. Alpine and Apennines mountain slopes represent the most vulnerable places of the country where shallow landslides and debris flow can occur more frequently (Ciccarese et al., 2020; Gariano and Guzzetti, 2016; Longoni et al., 2011; Montrasio, 2000; Montrasio and Valentino, 2016; Rossi et al., 2019; Vessia et al., 2014, 2016). We can cite several examples of past events such as the case of Valtellina (Lombardy) in 1987 as well as Piedmont in 1994 and 2000 and Genova ~~city~~ in 2011 and 2013 (Inventario Fenomeni Franosi; ISPRA, 2018). All of these catastrophic events have been caused by rather exceptional rainfall episodes that rarely occur and have particular features regards their durations and their intensities (Ceriani et al., 1994; Corominas et al., 2014; Guzzetti et al., 2007; Rappelli, 2008). Here, the scientific literature has proposed some analytical methods for relating the triggering event to the occurrence of rainfall-induced landslides.

A first methodology consists of the analysis of the rainfall return period (RP) for establishing the intensity of the meteorological trigger (Caine, 1980; Iverson, 2000). The RP has a statistical meaning and represents the average recurrence time of a rainfall episode characterized by a certain intensity (I) and duration (D), that happened at a specified location (Bovolo and Bathurst, 2012; Frattini et al., 2009; Iida, 2004). This information can potentially be linked to the recurrence of the eventually triggered ~~hydrogeological~~geo-hydrological phenomena in case we make the hypothesis of iso-frequency with the RP of precipitation (De Michele et al., 2005; ISPRA, 2018). For a flood or a flash flood, that approximation is generally acceptable because a inundation represents the direct consequence of a heavy precipitation (Albano et al., 2017a; De Michele et al., 2005). Instead, defining a RP for a landslide is not a common practice because the failure is not a periodic event but is a sudden collapse (ISPRA, 2018). For complex and deep-seated landslides the meteorological triggering factors are also intimately bounded with the local predisposing factors, i.e. the territory morphology, geology, etc. (Ciccarese et al., 2020; Guzzetti et al., 2007; Inventario Fenomeni Franosi; ISPRA, 2018; Longoni et al., 2016; Montrasio, 2000; Ozturk et al., 2015; Papini et al., 2017). The ~~rupture surface~~ position of the surface rupture and the seasonal groundwater circulation can have a crucial interplay role influencing the overall stability of the landslide (Longoni et al., 2014; Ronchetti et al., 2009; Xiao et al., 2020). Therefore, it is not always clear how to identify the real cause of the collapse and, the correlation with rainfall triggers is sometimes weak (Ibsen and Casagli, 2004).

A certain degree of reciprocity with precipitation triggers is maintained mainly for rainfall-induced events such as shallow landslides, soil slips, and debris flows. Therefore, a common methodology consists of the investigation of rainfall intensity-duration (I-D) curves (Ceriani et al., 1994; Ciccarese et al., 2020; Crosta and Frattini, 2001; Gao et al., 2018; Guzzetti et al., 2008; Longoni et al., 2011; Olivares et al., 2014; Peruccacci et al., 2017; Rappelli, 2008; Rosi et al., 2016; Vessia et al., 2014, 2016; Segoni et al., 2014). The rainfall thresholds are valid for a specific region where in respect to the duration and the intensity of the precipitation episode a shallow terrain movement could be triggered or not. These curves are created looking at the past events that occurred across a region, therefore, are site-specific (Ceriani et al., 1994; Guzzetti et al., 2008;

ha formattato: Italiano (Italia)
Codice campo modificato
Codice campo modificato
Codice campo modificato
ha formattato: Italiano (Italia)
Codice campo modificato
ha formattato: Italiano (Italia)
Codice campo modificato

Rappelli, 2008; Rossi et al., 2012). Intrinsically they include the susceptibility of the local territory to landslide failure so their use cannot be always extended to other regions with different geological and morphological characteristics (Caine, 1980; Guzzetti et al., 2007; ISPRA, 2018; Longoni et al., 2011; Peruccacci et al., 2017; Ozturk et al., 2018). Moreover, due to their empirical nature, I-D curves are sometimes rather approximate and could detect "false alarms" or, conversely, miss some "true alarms" (Abbate et al., 2019; Guzzetti et al., 2007; Peres et al., 2018). Some studies have demonstrated their dependency on the humidity condition of superficial terrain (Jie et al., 2016; Lazzari et al., 2018). This characteristic adds further uncertainties to the reliability of I-D method. However, the I-D thresholds are widely used in the field of ~~hydrogeological~~geo-hydrological risk prevention because permit to give a fast preliminary prediction of the occurrence of shallow soil failures in function of the local meteorological previsions (Piciullo et al., 2017).

Through the I-D threshold methodology, it is possible to distinguish critical events from non-critical ~~ones~~ones, but no further information can be retrieved directly about their magnitude. One possible solution is to try to integrate rainfall thresholds with the probability of temporal occurrence considering again the RP of the rainfalls, under the hypothesis of iso-frequency between the triggers and the ~~hydrogeological~~geo-hydrological effects: low magnitude events exhibit higher probabilities of occurrence while greater magnitude episodes have rare frequencies. In addition, I-D points that exhibit higher RPs are generally located at a higher distance from the I-D thresholds (Crosta and Frattini, 2001). This fact is explained by recalling the statistic of the precipitation extremes (De Michele et al., 2005) where for any fixed rainfall duration, the ~~increasing~~ increase of rainfall intensity determines an increase in RP. For these reasons, that "point-threshold" distance is related to the RP and in principle could be considered for a magnitude classification of the critical event identified. Unfortunately, this assumption is generally valid only for events recorded around a very limited area where precipitation statistics are supposed to be spatial invariant.

Up to this point, we have presented the most common strategies adopted for describing the precipitation characteristics in rainfall-induced ~~hydrogeological~~geo-hydrological events. In these methodologies only *I* and *D* parameters are investigated but are these methods enough~~sufficient~~ for a complete description of the rainfall triggering factors? Is RP a good predictor of their magnitude? Can rainfall analysis be improved considering also other meteorological variables that are related to the magnitude of the trigger? In our study, we have tried to answer these questions proposing an alternative of the conventional I-D rainfall analysis be able to classify rainfall events according to the spatial extent of their impact. We propose a reanalysis of past meteorological events which provoked ~~a number of~~several landslide events. We have investigated rainfall triggers not only considering local rain gauge time-series but also including a broader description of the events looking at meteorological reanalysis maps at a regional scale. The goal was to establish a magnitude ranking among the rainfall-induced ~~hydrogeological~~geo-hydrological events studied in order to identify the most critical ones. In this light, a ~~70~~ 70-year reanalysis study is presented starting from a group of past rainfall episodes that happened in the alpine region of northern Lombardy, Sondrio Province, Italy (Sistema Informativo sulle Catastrofi idrogeologiche; Inventario Fenomeni Franosi; Rappelli, 2008; Tropeano, 1997). Triggering factors are interpreted following two approaches:

ha formattato: Italiano (Italia)
Codice campo modificato
ha formattato: Italiano (Italia)
Codice campo modificato
ha formattato: Italiano (Italia)
ha formattato: Italiano (Italia)

- In the first approach, we put the events in the context of the classical I-D approach, integrated with the estimation of RP, as mentioned earlier. We then propose an alternative for the classification of the events' magnitude through the introduction of a magnitude index (MI). The index incorporates the return period of an event with the spatial extent of its impact in terms of landslide occurrence. The MI is defined in substitution of the classical magnitude quantification adopted for ~~hydrogeological~~geo-hydrological events (Corominas et al., 2014; Malamud et al., 2004).
- A second approach is based on a meteorological analysis of the triggers, considering their interpretation coming from the Norwegian Cyclone Model (NCM) (Godson, 1948; Martin, 2006; Stull, 2017). Here, the trigger's magnitude is expressed through a ~~physically~~ physically-based meteorological index called the "Sea Level Pressure Tendency" (SLPT) which is a function of some atmospheric parameters evaluated at the synoptic scale and associated with the rainfall event.

To carry out our study two data sources are considered:

- Ground-based meteorological series of rainfalls (Rete Monitoraggio Idro-nivo-meteorologico; SCIA: Sistema Nazionale per l'elaborazione e diffusione di dati climatici), adopted for I-D methodology and for the RP evaluation.
- Meteorological maps provided by the National Centres of Environmental Prediction (NCEP) (Kalnay et al., 1996; Observations, Prévisions, Modèles en temps réel; National Center for Environmental Information) for the NCM intensity assessment.

ha formattato: Italiano (Italia)

Codice campo modificato

ha formattato: Italiano (Italia)

ha formattato: Italiano (Italia)

The paper will be organized as follows: in section 2 is presented a brief description of the historical databases and the meteorological reanalysis maps; in section 3 are described the two methodologies behind the definition of the MI, through the extended rain-series analysis, and the SLPT, through the NCM model theory; in section 4 the outcomes from the two presented approaches are reported and the two indexes are then compared. A discussion is developed in section 5 with some comments about the obtained results, with a focus on the SLPT index performances; in the last section are reported some final remarks and conclusions of the ongoing research work.

2 Data and Materials

2.1 Historical database of ~~hydrogeological~~geo-hydrological events and rainfall Time Series

A group of past ~~hydrogeological~~geo-hydrological events has been considered from the alpine area of Sondrio Province, northern Lombardy, Italy, Figure 1~~Figure 1~~ . In our study, we have investigated historical databases to identify events that in the recent past exhibited similar cause-effect behaviour, like the 1987 event. In July 1987 this area was affected by exceptional ~~hydrogeological~~geo-hydrological events triggered by a rather intense and prolonged rainfall episode (Rappelli, 2008; Tropeano, 1997). The effects on the territory were severe: shallow landslides, debris flows, and flash floods were

recorded causing people injuries, 35 fatalities, and extended damages to infrastructure and buildings, estimated at 2 billion euros (Sistema Informativo sulle Catastrofi idrogeologiche).

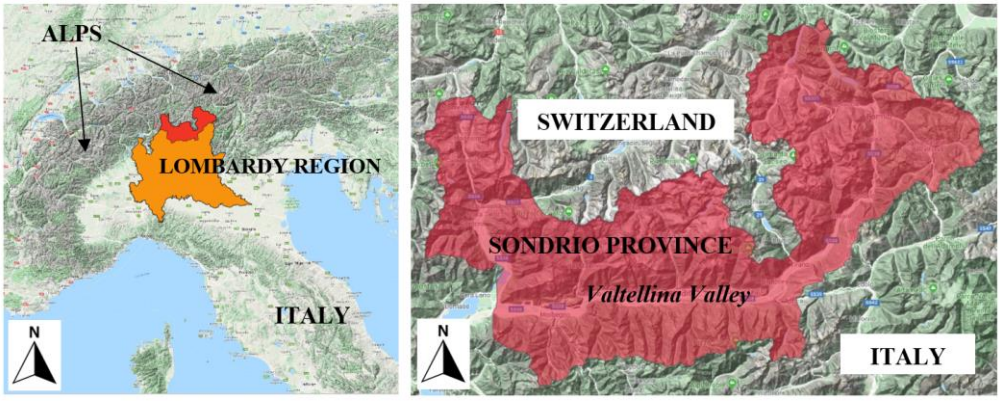

Figure 1: Case study area of Sondrio Province, northern Lombardy, base-layer from © Google Maps 2020.

Two different data sources were investigated to collect historical data: the "Aree Vulnerate Italiane" (AVI) database and the "Inventario Fenomeni Franosi Italiano" (IFFI) database (Sistema Informativo sulle Catastrofi idrogeologiche; Inventario Fenomeni Franosi). The data collect historical information from past natural disaster starting from the medieval age up to nowadays: the AVI database is directly available inside a geoportal-web site that is managed by CNR (Centro Nazionale della Ricerca) and the IFFI database, available from the national geoportal website (Sistema Informativo sulle Catastrofi idrogeologiche; Inventario Fenomeni Franosi). Available events time-series were not homogeneous so that the consistency of the database was evaluated, redundant records have been dropped and a final integration between the AVI and the IFFI database information was carried out.

The period chosen for the reanalysis is comprised between 1951 and 2019. Systematic monitoring of the precipitation and temperature started in Italy in 1951 by SIMN (Servizio Idrografico e Mareografico Nazionale) and looking at the antecedent periods these data were missed or characterized by several uncertainties or errors (SCIA: Sistema Nazionale per l'elaborazione e diffusione di dati climatici). The available rain gauge data series were gathered from local archives of SIMN (SCIA: Sistema Nazionale per l'elaborazione e diffusione di dati climatici) and ARPA Lombardia (Agenzia Regionale per la Protezione dell'Ambiente) (Rete Monitoraggio Idro-nivo-meteorologico). These series were conventionally recorded on daily basis until the 2000s years so "a daily rain" represents the maximum resolution of our dataset before that period. Starting from 2001, the available temporal resolution has moved to a sub-hourly time-step increasing the accuracy of the rainfall analysis.

In AVI and IFFI database, the precise ~~localization~~ location of ~~hydrogeological~~geo-hydrological episodes ~~was~~were not available even for the most recent events that happened after the 2000s. Therefore, some indications about locations were

retrieved from the AVI database considering the municipalities affected by disasters. The spatial extension of affected areas (AA) describe those locations that have experimented with some damages due to ~~hydrogeological~~geo-hydrological events that occurred. This information is indicative of the area where the rainfall event has been supposed to be more intense. In fact, AA was then compared with ground-based rain gauge series from the entire Sondrio Province with the aim to reconstruct~~ion~~ for each rainfall event its spatial distribution. Selected events have been classified in function of AA parameter: extremely localized events (EXL), with an influence area lower than 1000 km^2, or diffuse events (DIF), with significant territorial diffusion greater than 1000 km^2. This threshold has been motivated referring to the nature of the meteorological triggers: EXL were generally associated with convective rainfall phenomena which extension has an order of 10 x 10 km^2 and DIF were characterized by diffuse and uniform rainfall with an extension around 100 x 100 km^2 (Martin, 2006; Rotunno and Houze, 2007). In Table 1~~Table 1~~ is reported the list of ~~hydrogeological~~geo-hydrological events analysed in our study.

Codice campo modificato

Table 1: ~~Hydrogeological~~Geo-hydrological events recorded from 1951 up to 2019 considered for the back-analysis study. In the table are also reported the event classification considering their spatial extension; the extreme localized events (EXL) and the more diffuse ones (DIF). (*) uncertainty data.

YEAR	START	END	METEO TYPE	EFFECTS	MUNICIPALITY AFFECTED	AFFECTED AREA km²	EXTENSION TYPE	CUMULATED RAIN mm	EVENT DURATION hours
1951	7 august	8 august	Heavy rainfall	Flash Floods	4	800	EXL	218.0	48
1953	17 july	18 july	Heavy rainfall	Flash Floods	3	250	EXL	83.8	24
1960	15 september	17 september	Heavy rainfalls	Landslide and Floods	17	1500	DIF	115.6	48
1966	3 november	5 november	Prolonged rainfalls	Landslides and Floods	3*	1000	DIF	128.6	72
1983	21 may	23 may	Heavy rainfalls	Landslides	12	500	EXL	208.6	72
1987	16 july	19 july	Prolonged rainfalls	Landslides and Floods	77	3000	DIF	254.8	96
1997	26 june	29 june	Prolonged rainfalls	Landslides and Floods	6	500	EXL	275.0	96
2000	13 november	17 november	Prolonged rainfalls	Landslides	60	2000	DIF	218.7	96
2002	13 november	18 november	Prolonged rainfalls	Landslides	60	2000	DIF	308.8	120
2008	12 july	13 july	Heavy rainfalls	Landslides	6	300	EXL	60.0	12
2018	27 october	30 october	Prolonged rainfalls	Landslides	20	1500	DIF	242.4	96
2019	11 june	12 june	Heavy rainfall	Landslides and Floods	9	700	EXL	110.0	13

2.2 NCEP reanalysis maps

To improve the description of rainfall triggering factors, the meteorological reanalysis maps were examined considering the National Centre for Environmental Prediction (NCEP) data (Kalnay et al., 1996; Observations, Prévisions, Modèles en temps réel). The former has a spatial resolution of 2.5° x 2.5° degrees of latitude and longitude, covering the whole planet with a temporal frequency of 12 h. All the data stored in NCEP maps are useful for the interpretation of air masses dynamic in the middle latitudes such as the Extratropical Cyclones (ECs) that are responsible for the spatial and temporal evolution of intense precipitation phenomena. For the European region, ECs develops in the Atlantic Ocean near the British Islands. ECs are deputed for the large part of precipitation recorded over the Alps mountain range (Rotunno and Houze, 2007) because they are generally advected eastward through the Mediterranean area by Rossby waves (RW) (Grazzini and Vitart, 2015; Martin, 2006). At the boundary of the polar vortex, RW can generate strong jet streams that can move air masses in the direction of the southern Alps, enhancing vertical air motions. Across the southern flank of the Alps, this mechanism may lead to trigger persistent and heavy precipitation (Rotunno and Houze, 2007) that can intensify if an orographic uplift of the incoming southerly flow is also triggered (Abbate et al., 2021; Grazzini, 2007). Rainfall can reach remarkably high amounts if these conditions are prolonged for several days, leading up to 400 mm in 2/3 days (Grazzini, 2007; Rotunno and Houze, 2007). For each event listed in Table **1** ~~Table 1~~, we have examined correspondent NCEP maps to investigate the mechanism responsible for generating those intense precipitations over the target area.

3. Model and Methods

The triggers analysis is here presented considering the I-D thresholds approach, its extension through the MI index definition and the NCM model with SLPT index evaluation.

3.1 Rainfall I-D thresholds and Return Period analysis

The daily rainfall rate has been determined from the total amounts and the duration listed in Table 1. Rainfall amounts (RA) were estimated keeping the distinction between EXL and DIF events, Figure 2.A. For EXLs the nearest rain gauge or at least the 2 nearest rain gauges were chosen as reference. For DIFs, all the available daily rain data RA_i in the territory have been summed and averaged considering the number of rain gauges stations "n" to obtain a representative value for RA_{avg}, Eq. (1.a). We have assumed the hypothesis of a uniform spatial distribution of the rain gauge stations, Figure 2.B, neglecting any influence of elevation on rainfall data (Abbate et al., 2021). Then, RR was computed as the ratio of the cumulative rainfall RA_{avg} on the duration *D*, Eq. (1.b).

$$RA_{avg} = \frac{\sum_{i=1}^{n} RA_i}{n} \qquad expressed\ in\ mm \tag{1.a}$$

$$RR = \frac{RA_{avg}}{D} \qquad expressed\ in\ mm\ h^{-1} \tag{1.b}$$

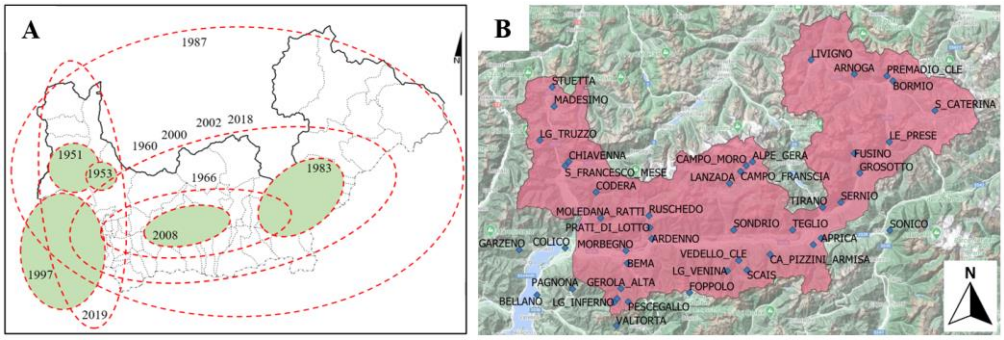

195 Figure 2: A) distribution of critical events across Sondrio province and B) the local rain gauge station network considered in the study, base-layer from © Google Maps 2020.

For the studied area, a set of thresholds proposed in the literature was considered, reported in Table 2. All the rainfall thresholds have a monomial expression where D is the duration of the rainfall (hours), and I is the average rainfall intensity (mm h^{-1}). The "Caine" curve (2.a) (Caine, 1980) is the most general one, valid worldwide for shallow landslides and debris 200 flow phenomena. At a regional scale, a more recent study conducted by (Guzzetti et al., 2007) proposed a new set of curves valid for central and southern Europe, considering a distinction among different climate types. In our study, three of them were selected: the general one (2.b), the curve valid for mid-climate (2.c), and the one suitable for highlands and mountain environments (2.d). Another study from (Peruccacci et al., 2017) further extended the previous study by Guzzetti addressing a new I-D threshold valid for the Italian country. At the local scale, the "Cancelli Nova" (2.e) (Rappelli, 2008), the 205 "Ceriani" (2.f) (Ceriani et al., 1994), and the "Crosta Frattini" curves (2.h) (Crosta and Frattini, 2001) were proposed respectively in 1985, 1994 and 1998. All of them were calibrated directly on the recorded data available in Sondrio Province.

Table 2: I-D threshold curve set considered in this study.

I-D THRESHOLD CURVES	AUTHORS	VALIDITY	EQUATION
$I = 14.84\ D^{-0.39}$	Caine	World	(2.a)
$I = 8.67\ D^{-0.61}$	Guzzetti	Regional (Italy)	(2.b)
$I = 18.6\ D^{-0.81}$	Guzzetti	Regional (Italy)	(2.c)
$I = 8.53\ D^{-0.64}$	Guzzetti	Regional (Italy)	(2.d)
$I = 7.70\ D^{-0.39}$	Peruccacci	Regional (Italy)	(2.e)
$I = 44.67\ D^{-0.78}$	Cancelli Nova	Local (Lombardy region)	(2.f)
$I = 20.01\ D^{-0.55}$	Ceriani	Local (Lombardy region)	(2.g)
$I = 12\ (D^{-1} + 0.07)$	Crosta Frattini	Local (Lombardy region)	(2.h)

For each event, the couple points *RR-D* were plotted against the I-D threshold curves, and their return period RP was evaluated. The former was determined following the methodology based on the IDF curves (Intensity Duration Frequency) (De Michele et al., 2005) available for the Lombardy region and provided by (Rete Monitoraggio Idro-nivo-meteorologico). The coefficients of IDF curves are estimated through the analysis of rainfall extremes addressing the GEV (Generalized Extreme Value) distribution. The dataset considered for the GEV was the SIMN time-series (SCIA: Sistema Nazionale per l'elaborazione e diffusione di dati climatici) gathered from 1960 up to 1990 across the whole territory of the region. Bearing in mind that our localized events EXL has been distinguished separately in respect to the diffuse DIF, also for the RP calculation, we have considered the same assumptions as for RR evaluation. For the localized events, the on-site coefficient of IDFs has been taken ~~directly~~, while~~but~~ for the diffusive ones, a spatially averaged value has been computed.

3.2 Trigger's hazard estimation and the MI magnitude index

A further step in the precipitation analysis consists of the hazard and magnitude assessment for each event. According to (Guzzetti et al., 2005) the general landslide hazard could be defined as a probabilistic function of three terms Eq. (2.a): the size A_l, the temporal occurrence T_l and the spatial susceptibility S. ~~In T~~the "size" term ha~~sve~~ stored the information about the volume, the area or the density of landslides occurred over a particular area. The temporal occurrence considers the periodical reactivation of a single landslide (deep-seated) or the recurrence of shallow landslides ~~episode~~ inside a catchment. The spatial susceptibility represents the quantification of the territory predisposition to a landslide phenomenon.

$$H_{landslide} = P(A_l \geq a_l) \cdot P(T_l \geq t_l) \cdot S \qquad 2.a$$

$$S = 1 \qquad 2.b$$

$$log\big(P(A_l \geq a_l)\big) = a - b\,AA \qquad where\ a, b\ are\ the\ coefficients \qquad 2.c$$

$$log\big(P(T_l \geq t_l)\big) = c - d\,RP \qquad where\ c, d\ are\ the\ coefficients \qquad 2.d$$

Starting from the definition of Eq.2.a. we have extended this concept and adapted it to interpret the events in our reanalysis study. The aim was to define a proper hazard and then a magnitude indicator for ~~the hydrogeological~~geo-hydrological events considering the temporal and spatial probability of occurrence of the triggering rainfalls. According to (Malamud et al., 2004) a scale for the magnitude is necessary to interpret quantitatively the episodes and to highlight the most severe ones. For landslides and rainfall-induced ~~hydrogeological~~geo-hydrological events, a unique method that describe the "energy" does not exist because several variables may play an important role in its definition (Bovolo and Bathurst, 2011; Frattini et al., 2009; Gao et al., 2018; Iida, 2004; Reid and Page, 2003). Therefore, under some hypothesis, we have proposed a new magnitude index (MI) as a quantitative parameter for assessing a proper magnitude ranking. Firstly, we have assumed that

the investigated area had a homogeneous susceptibility $S = 1$ to shallow landslide and debris flow triggering. This choice was motivated by geologicaly and morphologicaly features, also looking at recent susceptibility maps proposed by (ISPRA, 2018). Then we moved on other terms trying to determine the spatial and temporal probability of exceedance from AA and RP parameters, recalling the theory of frequency-magnitude relationship.

FrequencyThe frequency-magnitude curve (FMC) was proposed by (Gutenberg and Richter, 1944) for earthquake studies and then was also extended for interpreting different types of natural phenomena (Gao et al., 2019). The MCF curve is obtained by plotting incremental frequency F_i against the magnitude M_i on a logarithmic scale. F_i represents the frequency of the event that has a magnitude ≥ of a certain value M_i. In our study, the MFCs were considered to evaluate the probability of occurrence of a certain event in time and space and then combined in to determine its hazard as described in Eq. (2.a). The temporal occurrence term requires the estimation $P(T_l \geq t_l)$ from RP's frequency-magnitude relationship. This represents the probability of occurrence of an event T_l with a RP $\geq t_l$. According to (Guzzetti et al., 2005), the other hazard component is addressed by the landslide size, Eq. (2.d). In this regard, inside our database was not possible to retrieve enough sufficient information about event features, such as the volumes and areas involved or the numbers of landslide failures. Therefore, the AA parameter was used as a proxy of the "trigger's size" and was treated similarly to the RP term. The probability of spatial occurrence $P(A_l \geq a_l)$ of an event A_l with a AA $\geq a_l$, was retrieved from FMC, Eq. (2.c). Then, the hazard has been estimated using the Eq. (3.a). Due to the modification of the first term $P(A_l \geq a_l)$ it not properly represents the landslide hazard, but $H_{trigger}$ is an indicator of the hazard as a function the trigger's temporal frequency and spatial extension.

In most of the natural cases, the frequency of low magnitude hydrogeologicalgeo-hydrological events is rather high and vice-versa. Therefore, we tried to estimate the trigger magnitude as an inverse function of the hazard. The former is a combination of two probabilities of occurrence Eq. (3.b), therefore it can be transformed into a magnitude recalling again the FMC in Eq. (3.c). Working out some algebra with Eq. (3.a, 3.b and 3.c) we have obtained a representation of the magnitude expressed by the index MI, Eq. (3.d). The MI is a sum of two contributes: the first describes its spatial extension through the parameter AA and the second its temporal occurrence through the RP. In this light, the MI calculated was intended to be more complete rather than the single RP because through AA term it is possible to considers the "integral effects" related to the trigger's extension. The MI was taken as a reference for testing the SLPT index presented in the next section.

$$H_{trigger} = P(A_l \geq a_l) \cdot P(T_l \geq t_l) \quad 3.a$$

$$H_{trigger} = exp(a - b\,AA) \cdot exp(c - d\,RP) \quad 3.b$$

$$M_{trigger} = -log(H_{trigger}) = -log(exp(a - b\,AA) \cdot exp(c - d\,RP)) \quad 3.c$$

$$MI = M_{trigger} = -((a - b\,AA) + (c - d\,RP)) \quad 3.d$$

3.2 NCM model and SLPT index

The extratropical cyclone dynamic influences the rainfall intensities ~~recorded~~: if the EC is stronger, more precipitation is expected over an area but, depending on EC spatial and temporal evolution, rainfalls could exhibit different total amounts and duration. Therefore, using the NCEP maps, the Norwegian Cyclone Model (NCM) (Godson, 1948; Martin, 2006; Stull, 2017) was chosen for estimating a strength index of ECs. NCM was formulated in the early 20th century. It describes an extratropical cyclone that develops as a disturbance along the boundary (front) between the polar and mid-latitude air masses. The model calculates indirectly the Sea-Level Pressure Tendency (SLPT), the time-variation ratio of sea-level atmospheric pressure $\Delta p_{sl}/\Delta t$ (hPa h^{-1}) that represents an indicator of the strength of a cyclone structure (Andrews, 2010; Godson, 1948; Martin, 2006; Stull, 2017; Wallace and Hobbs, 2006). When the EC is more intense, the absolute value of the SLPT ratio is higher and, consequently, the EC can cause more rainfalls. According to (Stull, 2017), this index is obtained as a sum of four different influencing factors that correspond to the processes implicated in the dynamic evolution of extratropical cyclone:

$$\frac{\Delta p_{sl}}{\Delta t} = T_1 + T_2 + T_3 + T_4 = SLPT \quad (4)$$

- T_1 expresses the "upper layer divergence mechanism" due to jet streams, which removes air mass from the air column. In the Eq (4.a2), $\rho_{MID} = 0.5\ \mathrm{kg\ m^{-3}}$ is the average density of air column and $g = 9.8\ m\ s^{-2}$. W_{MID} $(m\ s^{-1})$ is the mean air column vertical velocity that is evaluated considering the Eq. (4.a1) in the proximity of the local change of jet stream velocity gradient $\Delta W_{js}(m\ s^{-1})$, where $\Delta z \cong 5000$ m and Δs_1 (m) jet streak elongation. According to (Stull, 2017), Eq. (4.a1) is a strong approximation because supposes air density constant over air column, so that we have considered a revised version (Stull, 2017) that expresses the W_{MID} in function of other parameters such as the geostrophic wind velocity $G(m\ s^{-1})$, the curvature radius R (km) of Rossby waves and Coriolis parameter $f_c(s^{-1})$;

$$W_{MID} = \frac{\Delta W_{js}}{\Delta z/\Delta s_1} \quad (4.a1)$$

$$T_1 = -\,g\,\rho_{MID}\,W_{MID} \quad (4.a2)$$

- T_2 is the "atmosphere boundary layer pumping", which causes the horizontal wind to spiral inward toward a low-pressure centre. In Eq. (4.b2), the air density of the boundary layer is $\rho_{BL} = 1.112\ kg\ m^{-3}$. $W_{BL}(m\ s^{-1})$ is the vertical velocities at boundary-layer calculated through Eq. (4.b1) following the approach proposed by (Stull, 2017) for cyclone structures: the b_{BL} factor is a function of boundary layer thickness, that can be assumed equal to 1000 m on average, and drag coefficient $C_d \approx 0.005$ is defined for flow over land;

$$W_{BL} = \frac{2\, b_{BL}\, C_d}{f_c} \frac{G^2}{R} \quad (4.b1)$$

$$T_2 = g\, \rho_{BL}\, W_{BL} \quad (4.b2)$$

- T_3 expresses the horizontal air mass advection that moves a low-pressure centre in the direction of the target region, Eq. (4.c2). The advection velocity M_c $(m\ s^{-1})$ is a function of the celerity of Rossby waves c_{RW} $(m\ s^{-1})$ and the geostrophic wind G, Eq. (4.c1). The spatial pressure gradient at sea level is evaluated considering the distance $\Delta s_2 (m)$ between the low-pressure centre and the target region;

$$M_c = c_{RW} - G \quad (4.c1)$$

$$T_3 = -Mc \frac{\Delta p_{GW}}{\Delta s_2} \quad (4.c2)$$

- T_4 is the "latent heating" due to water vapour condensation in rainfall. It comes from the theory of thermodynamic transformations of water vapour in the atmosphere where all the parameters for rain condensation processes are stored in the term b_{AD} . The precipitation that does reach the ground is related to the net amount of condensational heating during time interval Δt by Eq. (4.d1) where T_v (K) is average air-column virtual temperature, $a = 10^{-6}\ km\ mm^{-1}$, Δz (km) is the depth of the air column, the ratio of latent heat of vaporization to the specific heat of air is $Lv/Cp = 2500\ K\ kg_{air}\ kg_{liq}^{-1}$, and where ρ_{air} and ρ_{liq} are air and liquid-water densities, respectively, with $\rho_{liq} = 1000\ kg\ m^{-3}$. The hypsometric equation relates to pressure-temperature changes as reported in Eq (4.d2). For an air column with an average virtual temperature of $Tv \approx 300\ K$, we obtain $b_{AD} = 0.082\ kPa\ mm^{-1}$ in Eq (4.d3) that is considered for the description of the net column-average effect.

$$\frac{\Delta T_v}{\Delta t} = \frac{a}{\Delta z} \frac{L_v}{C_p} \frac{\rho_{liq}}{\rho_{air}} RR \quad (4.d1)$$

$$\frac{\Delta P_s}{\Delta t} = -\frac{g}{T_v} \frac{L_v}{C_p} \rho_{liq} RR = -b_{AD}\, RR \quad (4.d2)$$

$$T_4 = -b_{AD}\, RR \quad (4.d3)$$

When the balance in Eq. (4) is negative the cyclogenesis occurs. T_1, T_3, and T_4 bring a negative contribution ~~to the balance~~ strengthening the EC cyclogenesis and lowering the SLPT index. Instead, T_2 has a positive contribution and tends to weaken the ECs structure increasing SLPT value. In ~~Figure 3Figure 3.Aa~~ and ~~Figure 3Figure 3.Bb~~ have depicted the mechanisms described by four terms T_i. ~~Figure 3Figure 3.Cc~~ reports how the model works considering the contribution of each four components across the timeline (A to G) that represents the sages of EC: EC's formation phase (i.e. cyclogenesis) is from A to D stages and EC's dissipation phase (i.e. cyclolysis) is from D to G. The critical phase of the EC is in the proximity of

point D where negative terms overcome the positive one. The SLPT index has been evaluated in correspondence ~~of~~ with C / D stages.

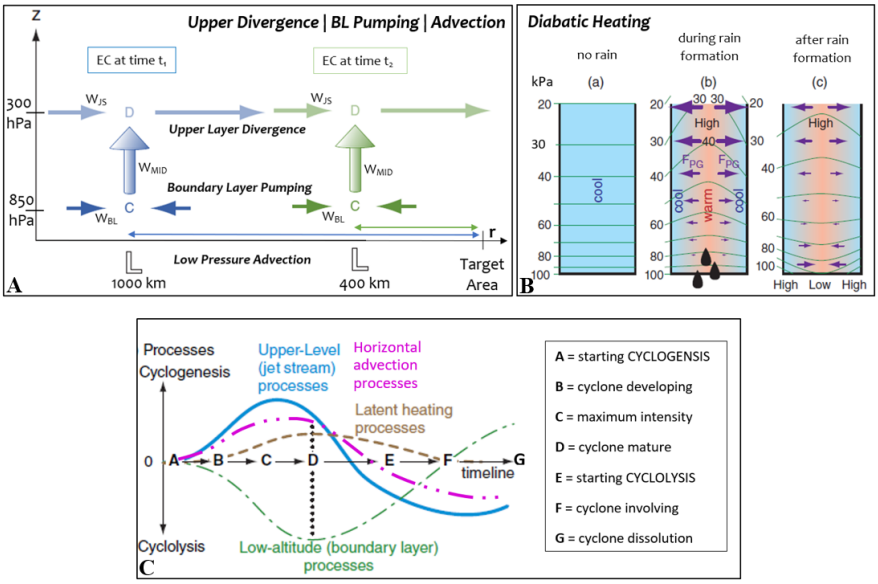

Figure 3: A) scheme of the mechanism represented by T_1, T_2, and T_3 terms, B) scheme of the mechanism represented by T_4 term, and C) qualitative temporal evolution of each of four terms T_1, T_2, T_3, and T_4 during cyclone phases (A to G) and their contribution to cyclone formation (cyclogenesis) and cyclone dissolution (cyclolysis), ~~proposed in (Stull, 2017),~~ modified after (Stull, 2017),.

4 Results

In this section the results are presented ~~the results~~ in four steps. Firstly, ~~is reported~~ the qualitative analysis coming from the direct interpretation of database and NCEP maps is reported. Secondly ~~is carried out~~ the I-D rainfall analysis is carried out and the MI index evaluation is described. Thirdly ~~is estimated the SLPT~~ for each considered event the SLPT is estimated and then compared ~~with~~ MI index.

4.1 Database interpretation and NCEP maps

The dataset of Table 1~~Table 1~~ shows a clear seasonal distribution of the events mainly concentrated during summer and autumn seasons. July and November are the months more prone to ~~hydrogeological~~geo-hydrological events and this strong seasonality highlights that the triggers phenomena involved may have a different origins~~nature~~ (Martin, 2006; Rotunno and Houze, 2007). In July, meteorological events are characterized mainly by high intensity and short duration with a typical

Codice campo modificato

convective behaviour of precipitation (thunderstorms), and their average duration is generally around 1 or 2 days. In particular, 1951, 1953, 1987, 1997, 2008 and 2019 events happened during the summer season and rainfall cumulated were comprised between 100-200 mm, apart from 1987 and 1997 that were rather exceptional (254 mm and 275 mm in three days ~~on average~~). During October and November, rainfall events are characterized by higher persistency (4-5 days) and rainfall cumulated can easily reach amounts around 250-350 mm, such as for the events that happened in 2000, 2002, and 2018.

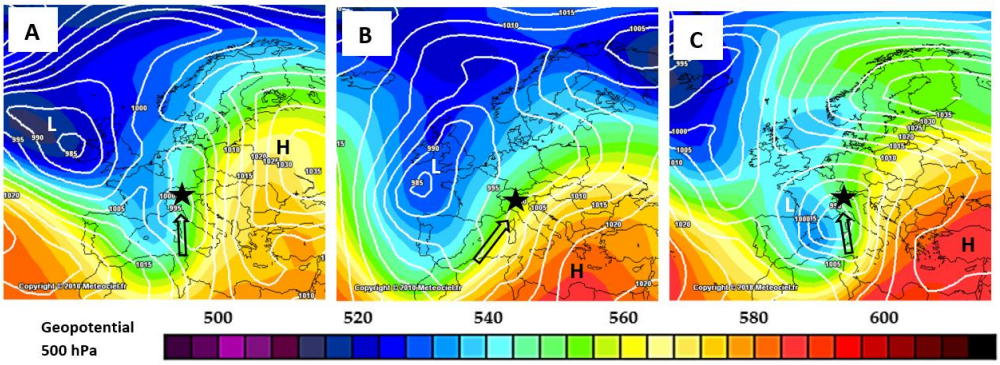

Figure 4: Reanalysis maps from NCEP reporting the Sea-Level Pressure and 500 hPa Pressure (colours) for 1966 A), 2002 B) and 2018 C) events where the black star is the Sondrio Province position, and the black arrow indicated the incoming southerly flow responsible of huge precipitation enhancing, adapted from (Meteo Ciel, 2020), modified after

Through the analysis of NCEP maps, we have observed that all the events reported in Table 1~~Table 1~~ have been ~~all~~ triggered in correspondence of EC structures that moved eastward from the Atlantic Ocean in the direction of the Alpine mountain range. In Figure 4~~Figure 4~~ are reported three examples of reanalysis maps that show the pressure distribution at 500 hPa reference height across Europe during the 1966, 2002 and 2018 events. A qualitative comparison among the three maps highlights that three events have been characterized by the evolution of a rather intense EC that is recognizable from the deep low pressure (L) located near the British Islands. This recurrent configuration has been responsible for the torrential rainfall recorded in the ~~southern~~ Southern Alps across the Sondrio Province. Consequently, the ~~hydrogeological~~geo-hydrological effects ~~triggered~~ could be directly imputed to the intensification of these EC structures. Starting from this qualitative evidence we have moved to a quantitative analysis following the two approaches proposed.

4.2 Approach 1: I-D threshold rainfall analysis and MI index extension

The average daily rain rate *I* and the duration *D* of the rainfall episodes in Table 1~~Table 1~~ were plotted against the rainfall threshold curves listed from Eq. (2.a) to Eq. (2.f) inside ~~Figure 5~~Figure 5. Most events can be clustered in the right-bottom corner of the graph due to their characteristics of a rather long duration of 2-4 days and slightly low intensities. Only the event of 2019, 2008 and 1953 are dispersed on the other side of the graph where the duration is around or less than a day.

Considering the thresholds proposed by Guzzetti, all the events ~~points~~ are correctly settled above. No ~~significative~~ significant differences are seen among the general one (b), the curve valid for mid-latitude climate (c) and the one valid for highlands climate (d). Peruccacci (e) and Crosta-Frattini (h) pose~~s~~ intermediately between the regional threshold of Guzzetti and the local ones proposed by Cancelli-Nova (f) and Ceriani (g). It seems that Guzzetti, Peruccacci and Crosta-Frattini may overpredict critical events because they are positioned rather low, especially for short duration ones.

The thresholds proposed by Caine (a), Cancelli-Nova (f) and Ceriani (g) are placed above the previous ones. The Ceriani curve ~~one~~ seems to fit very well the data, positioning only the 1966 event slightly below the curve and the 1953 and 1960 close to the curve. Also, Cancelli Nova works rather well posing only 1953 below the threshold. These results were expected because both (g) and (f) threshold were calibrated using a local dataset, respectively up to 1985 and 1994. Conversely, the Caine threshold seems to work worst rather than the previous leading to underprediction: 1953, 1960 and the 1966 events are not identified as critical and appear below the curve. Moreover, the 1997 and 2000 are settled borderline on the curve.

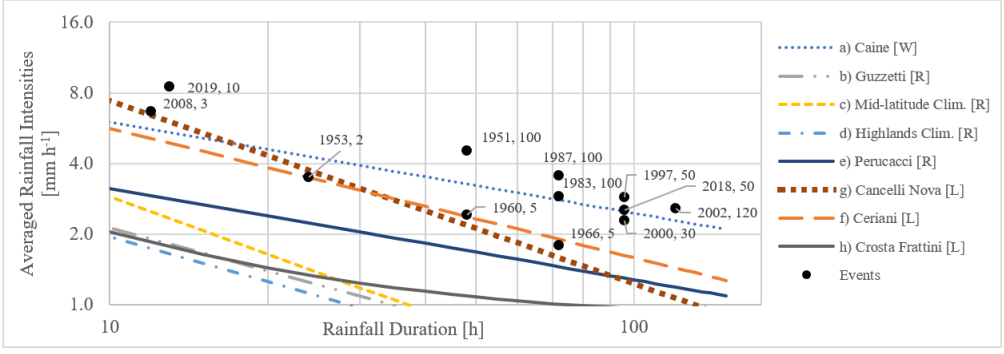

Figure 5: Intensity-Duration thresholds for considered events and relative rainfall RP.

The threshold curves analysed have divided our events into critical and non-critical ones but no further information on their magnitude ~~were~~ was retrieved yet. Some authors have shown that a measure of ~~that~~ magnitude may be established considering the relative distances between the I-D points and the threshold curve. According to (Crosta and Frattini, 2001; Gao et al., 2018; Iida, 2004; Rosso et al., 2006), a beam of rainfall I-D curves can be elaborated including their dependence ~~from~~ on RP. For ~~a~~ the same area, rainfall events with higher RP should be statistically located much more distant from the threshold lines, but this fact strongly depends on the reference curve considered as the lower bound. In our study, local

thresholds of Ceriani and Cancelli-Nova have demonstrated to best fitting the dataset avoiding under- and over predictions. Moreover, they are delimited by 1953, 1960, 1966 and 2008 events which exhibit the lowest RPs comprised between 2-5 years. Taking these curves as a reference we can appreciate that other critical events showing higher RPs are also located at more distance from these curves. This represents a confirmation of what found in the literature, but, in our opinion, the magnitude assessment looking simply at relative threshold distance seems rather approximate. In fact, the RP estimation depends not only on rainfall I-D values but also on parameters of GEV that takes into account the spatial variability of local precipitation statistics (De Michele et al., 2005). In those cases where rainfall intensity and duration are fixed, changing the GEV parameters also the RP may vary even though the relative distance from the curve is ~~maintained~~ the same. In our dataset, we have encountered this fact two times comparing 1983 and 1987 events, and 1997 and 2018 events that respectively exhibit the same RP with the same duration but a different relative distance from the curves. As a result, these distances could be used as a proxy of the magnitude only for rainfall analysis carried out at the same location where the GEV parameters remain constant, confirming what suggested by other authors. In our case study, this condition was not satisfied because the GEV parameters were not constant in space.

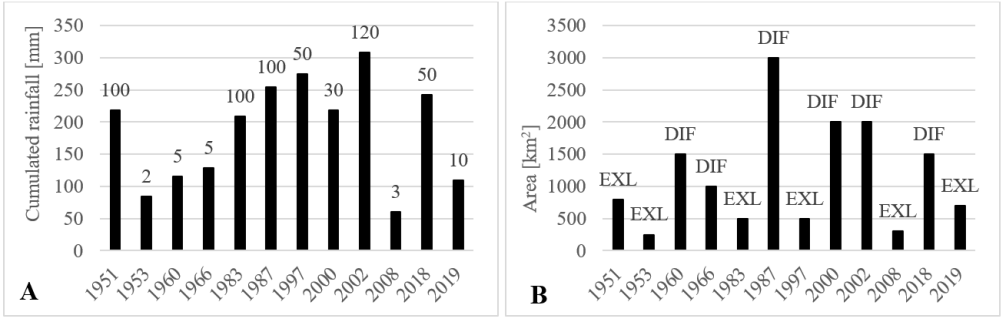

Figure 6: Cumulated rainfall and RP of triggering events A) and the Area affected by ~~hydrogeological~~geo-hydrological issues B).

Looking at ~~Figure 6~~Figure 6.A, the Sondrio Province has experienced at least four exceptional rainfall events with a return period equal to~~,~~ or higher than 100 years~~ -~~: 1951, 1983, 1987 and 2002. From RP analysis, they were ranked with the same intensity but among them, 1987 has been recorded historically as the most catastrophic one that affected the area in the second half of the XX century. This apparent contradiction has a possible explanation if we also include the information about the spatial extension of the triggers, as reported in ~~Figure 6~~Figure 6.B, which is a property strictly related to the nature of the rainfall event (Corominas et al., 2014; Gao et al., 2018). This parameter is not explicitly considered in RP evaluation. As an example, we can compare the 1983 and 1987 events. If only the RP is considered, 1983 intensity is equal to 1987, but considering the spatial distribution, the 1983 event affected only a limited area while 1987 spread across the entire province. For this reason, if we are interested in determining the magnitude of meteorological triggers, 1987 should be intended ~~worse~~ more critical rather than ~~in~~ 1983. In this regard, the RP information could be misleading.~~,~~

According to (Corominas et al., 2014; Guzzetti et al., 2005) and following the methodology proposed in Eq. (2 to 3) we have moved further considering both RP and AA for determining the trigger's hazard and magnitude. First of all, the FMCs have been established, allowingpermitting us to define the probability of spatial and time occurrence as a function of parameters AA in Figure 7Figure 7.A and RP in Figure 7Figure 7.B. Secondly, AA has been plotted against the RP in Figure 8Figure 8.A and was observed their low statistical correlation. Then, considering the Eq. (3.a), the trigger's hazard has been defined and reported in Figure 8Figure 8.B. We can notice that the trigger's hazard is higher when higher are the probabilities of spatial and temporal occurrence. In particular, 1953, 2018 and 2019 represent the most hazardous events with lower RP and AA. On the other hand, 1987 and 2002 represent the lowest hazardous events because, from a probabilistic viewpoint, they exhibit both the highest return period and extension. Applying the Eq. (3.c) the trigger's hazard has been translated into the magnitude index MI, normalized in respect to its maximum and shown in Figure 8Figure 8.B. We can notice that the MI has highlighted the 1987 and 2002 as the most severe events. On the other hand, the 1953 and 2008 were depicted with the lowest magnitudes. An intermediate magnitude ranking was assessed for 1951, 1983, 1997, 2000 and 2018 events confirming historical evidence.

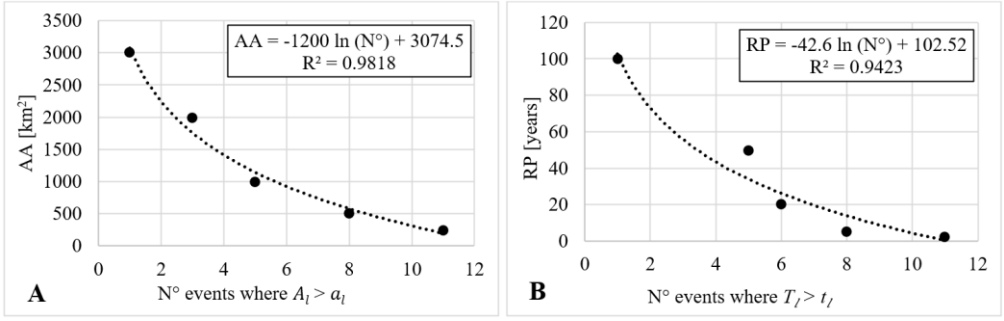

Figure 7: Frequency-magnitude relationship for A) Area Affected (AA) parameter and B) Return Period (RP) parameter.

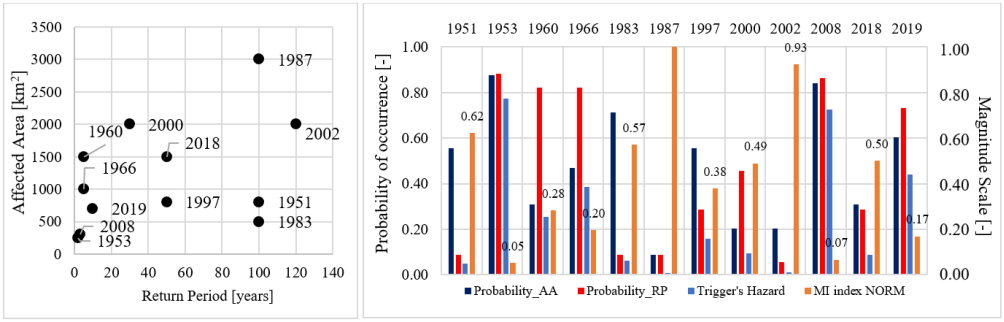

Figure 8: A) Correlation between RP and AA parameters, and B) determination the probability of occurrence of AA, RP and the Trigger's Hazard for dataset events

4.3 Approach 2: ECs intensity analysis and SLPT index

In the second approach, we applied the NCM described in Eq. (4). Using the NCEP data, atmospheric pressure gradients, wind velocities, and air masses advection through the Alpine region the model components in the Eq. (4.a2), (4.b2), (4.c2) and (4.d3) were studied.

For determining the T_1 term (Eq. 4.a2, upper layer divergence), the geostrophic wind velocities were estimated. Geostrophic wind is the theoretical wind that would result from an exact balance between the Coriolis force and the pressure gradient force. It represents a first approximation of the general circulation of the air masses at a regional scale. ~~and I~~intense geostrophic velocities are generally associated with strong EC structures (Andrews, 2010; Martin, 2006; Stull, 2017). As reported in ~~Figure 9~~Figure 8.A, geostrophic velocities were higher for 1983, 1987, 2000 and 2002, a sub-group of the most intense events of our dataset. Upwind velocities in ~~Figure 9~~Figure 8.B are also correlated with the presence of sustained geostrophic winds. Again 1987, 2002 and now 2018 have shown the highest values of the entire dataset.

For determining the T_2 and T_3terms (Eq. (4.b2) boundary layer pumping and Eq. (4.c2) advection), the air masses evolution paths were examined. ~~Figure 9~~Figure 8.C shows the short distance Δs_2 between the low pressure (L) and the Sondrio Province. We can notice that the relative position of ECs does not vary too much, 1183 km on average. This represents a characteristic of the ECs structures that tends to evolve across the Mediterranean and the Alpine area similarly. Nevertheless, some seasonal changes can be appreciated by looking at the advection path followed by the low-pressure centre (L). The larger part of the autumnal events exhibits a meridian motion of the low pressure from the northern part of Europe (Northern Sea) to the southern part, entering the Mediterranean Sea and moving eastward following Rossby waves track (Rotunno and Houze, 2007; Stull, 2017). This is the case of 1960, 1966, 2000, 2002 and 2018 events that occurred between September and November. Summer events of 1951, 1953, 1987, 1997 and 2019 exhibit a low-pressure tracking path that did not cross the Alps mountain range. This fact can be explained by considering that Rossby waves are in general shifted northward during

the summer period (Grazzini and Vitart, 2015; Martin, 2006). This reflects on the events that affect the southern side of the alpine region which are more rapid, less persistent, locally intense but not well organized such as the typical autumnal EC.

The T_4 term is represented by a linear function of the daily rainfall rates RR considered in the precipitation analysis. In the formulation adopted we made strong assumptions to yield the problem more tractable. This is the only component that depends on the accurate estimation of the ground-based rainfall data.

After calculating the intermediate components T_1, T_2, T_3 and T_4 terms, the Sea-Level Pressure Tendency index (SLPT) of Eq. (4) has been determined, Figure 9.D~~Figure 9~~. Firstly, we can notice that all these ECs have been characterized by explosive cyclogenesis. This definition applies when an extratropical cyclone exhibits a low pressure deepening of 24 hPa in 24 h, which corresponds to an average rate of 1 hPa h^{-1} (Sanders and Gyakum, 1980). Looking at Figure 9.D~~Figure 9,~~ the SLPT index shows a range comprised between the – 2.64 hPa h^{-1}, recorded for the 1953 event and -4.89 hPa h^{-1} recorded for 1987. The latter and 2002 (-4.67 hPa $^{-1}$) are reported to have been the EC structures with the highest intensity that affected the Northern Lombardy area. An average value of the SLPT index is reported around -3.67 ± 0.63 kPa h^{-1} that is compatible with the ECs structures shown by NCEP maps.

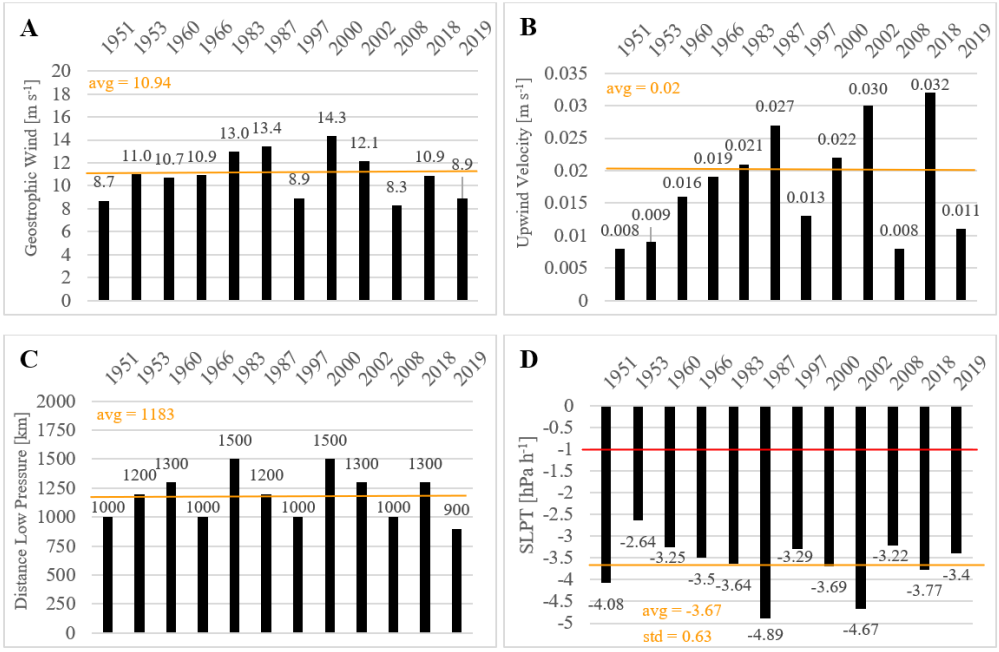

Figure 9: A) Upwind velocity and B) geostrophic wind velocity calculated for T_1 term and C) Δs_2 considered for T_2 and T_3 terms. D) The Sea-Level Pressure Tendency Index (SLPT) for the event analysed is compute. Orange lines represent the averages across the dataset while the red line indicates the threshold of explosive cyclogenesis (1 hPa h^{-1}).

4.4 Comparison between MI and SLPT indexes

The two methodologies proposed for the trigger's magnitude assessment are now compared. The two indexes MI and SLPT have been firstly normalized in respect to their maximum and then shown in ~~Figure 10~~Figure 10.A. We can observe that it is rather clear how the two indexes give a similar magnitude rank for the events examined in our dataset. Looking at bias errors, the mean absolute error (MAE) is computed around 7 % and the root mean square error (RMSE) is also about 10.3 %. The highest absolute error values were addressed by the 2008 and 2019 events. Moreover, we can show that two indexes are in accordance identifying 1987 as the episode with the highest magnitude, followed by 2002 and 1951. The lowest ranking scores are established for the 1953 event and 2008 that were already spotted by I-D analysis as borderline for Cancelli-Nova and Ceriani thresholds. In the middle, we found 1960, 1966, 1983, 1997, 2000, 2018 and 2019, ~~that~~ which were depicted also by historical chronicles as rather intense but not catastrophic for the Sondrio Province. ~~On~~ In ~~Figure 10~~Figure 10.B the MI index and the SLPT index have been plotted against each other. From the figure can be appreciated that the points lay on the diagonal and the correlation index R^2 is about 0.88, ~~that~~ which is rather high and near to 1.

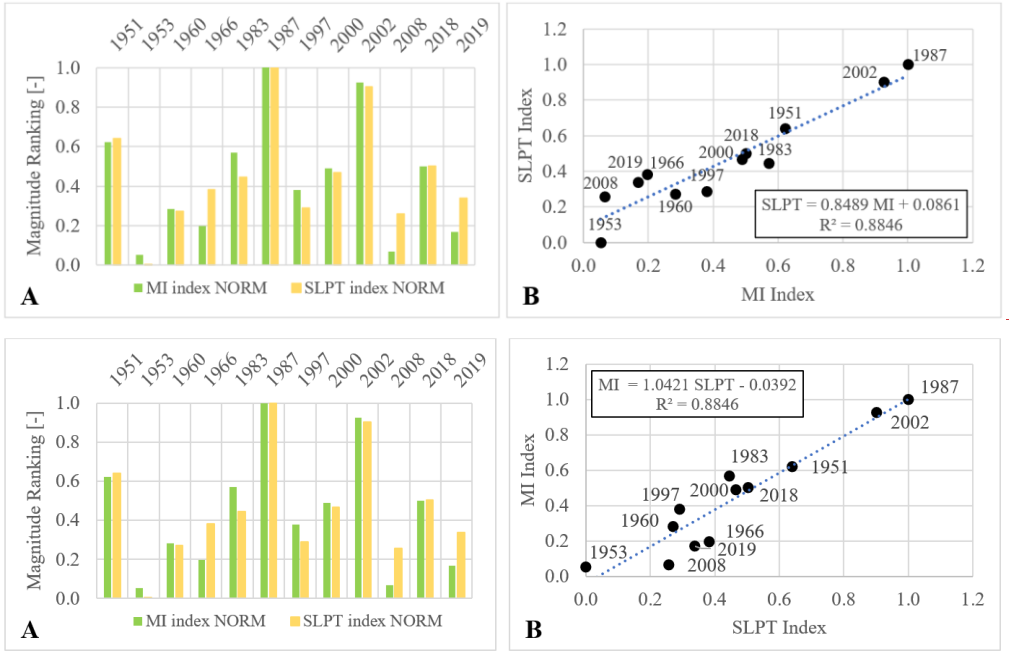

Figure 10: Comparison between MI index and SLPT index, normalized. The events recorded in 1951, 1987, 2002 and 2018 has highlighted with the highest magnitude while 1953 and 2008 events have the lowest values.

5. Discussion

Considering the results obtained, we discuss here the questions that aimed at our study. The first was: "Are the I-D thresholds and the RP evaluation enough~~sufficient~~ for a complete description of meteorological triggering factors?" The I-D thresholds are typically used for ~~hydrogeological~~geo-hydrological risk assessment but some uncertainties about their reliability have risen around two aspects: the choice of the ~~best~~ best-fitted threshold and the threshold's dependency on the RP parameter.

Regarding the first aspect, the thresholds ~~are able to~~can distinguish critical or non-critical events giving only a binary outcome of the event classification. Shifting up – down the curve or changing the curve, the same event can be detected respectively as a false negative or a false positive and this fact ~~that~~ may lead to a prediction error. In the specific case of our dataset, Guzzetti, Perrucacci and Crosta-Frattini curves seem to overpredict these~~at~~ events~~occurrence~~ while Caine was found to underpredict them~~it~~. On the other hand, Cancelli-Nova and Ceriani have demonstrated more suitable for interpreting our

dataset. In this regard, the local thresholds seem to be more accurate rather than the regional ones, but uncertainties remain about their correct application and interpretation. In fact, some recent studies have suggested that further investigation around their parameter's definition are required ~~in order~~ to improve detection performances. According to several authors (Bogaard and Greco, 2018; Kim et al., 2020; Lazzari et al., 2018) the threshold may exhibit ~~a~~ dynamic behaviour, shifting up-down ~~in function of~~considering the soil moisture and the antecedent cumulated rainfall especially for short duration events. This important condition has been normally neglected in the past definition of the thresholds, treating all the triggering events as uniform from the statistical point of view. Therefore, a wise disaggregation of these events in the function of antecedent conditions should be applied for creating a new threshold set that highlight the sensibility to those variables. In our opinion, this may help to improve further the performance of I-D methodology especially for locally based thresholds under the reasonable hypothesis of a uniform spatial susceptibility of the territory. On the other hand, for the regional ones, we think that the improvements would be less effective because also other factors related to the more heterogeneous area, such as morphological or geological predisposing causes, may play a more important role (Peruccacci et al., 2017). Including the RP in the threshold analysis can be useful to determine a preliminary magnitude ranking. Even though higher RPs are generally founded at a higher distance from the curve, the relative distance among I-D point and the reference threshold cannot be always considered as a proxy of the event magnitude. According to (Gao et al., 2018) this assumption~~relation~~ has been reported not so strong, and this was confirmed also in our reanalysis study. A possible explanation can be found in the way ~~of~~ the RPs are estimated. In principle, this interpretation of the trigger's magnitude is still valid only at a very local scale but cannot be adopted in our study since the GEV parameters used in RPs have changed in each rainfall episodes. Our results have highlighted this fact two times showing different point-threshold distances ~~in~~ with respect to the same RP values. In this perspective, ~~the~~ climate change will pose some challenges about the GEV updating for the future, considering that no stationary processes could affect the statistical distribution of critical precipitation (Albano et al., 2017b; Gariano and Guzzetti, 2016). This may add further uncertainties to this interpretation that considers only I-D thresholds and RPs for event magnitude estimation.

These two important observations represent a critical point in the I-D threshold methodology that has driven us to ask: "Is RP a good predictor of the magnitude?" Typically, the magnitude of a rainfall episode is described by the RP value, but this information is evaluated only ~~in~~ from time perspective. Taking inspiration from the landslide hazard definition proposed by (Guzzetti et al., 2005) we defined a new magnitude index, MI, that was also representative of the "triggers energy". In the definition of MI, we have included the information about the trigger's spatial distribution AA. This choice was aimed ~~by~~ at the lack of precise data about the landslide volumes, extensions, or numbers, ~~that~~ which are quantities considered for assessing an event magnitude scale (Malamud et al., 2004). The AA parameter can be interpreted as another proxy of the trigger's magnitude because indirectly it can describe the nature of the rainfall phenomena, distinguishing between a heavy thunderstorm, localized, in respect to a persistent ~~a~~ rain, more diffused. As shown by our results, RP and AA were uncorrelated so both were considered for the assessment of the magnitude index MI. The MI index was estimated in our study with post-event information but theoretically the index can be evaluated using weather forecasting, looking at expected

rainfall rates and amounts across different areas. In this regard, Local Area Meteorological Models (LAMs) can be used to estimate the MI index some hours in advance of the event ~~starting~~. In our opinion, this represents one of the main advantages of using MI because, in respect to the other magnitude indexes that requires precise information about the "post-failure" effects (number of triggered landslides or peak discharge), the MI can be established using again only meteorological information, much like the SLPT index that we propose further.

As a matter of fact, we have implicitly answered ~~to~~ the third question proposed: "Can rainfall analysis be improved considering also other meteorological variables that are related to the trigger's magnitude?" The assessment of the MI index has highlighted that the very local information about precipitation is not exhaustive, and ~~a~~ spatial distribution of the rainfall is also needed ~~for~~ to better comprehend the differences among the events. Moreover, if we are interested in the accurate trigger's description, looking only at the "final product" of a more complex meteorological process may be not enough (Monitoring European climate using surface observations; Rotunno and Houze, 2007; Stull, 2017). This is particularly true in mountain areas where the territory enhances the heterogeneity of the rainfall field (Abbate et al., 2021). For these reasons, other meteorological variables should be taken into account and included in the analysis. In our study, to pursue this goal we moved from a local perspective to a more regional one. This is crucial because it permits to better describe the different precipitation type that may influence the occurrence of ~~hydrogeological~~geo-hydrological failures (Corominas et al., 2014; Guzzetti et al., 2007). As an example, an intense thunderstorm during summertime could trigger few shallow landslides or debris over a limited area (Abbate et al., 2021; Montrasio, 2000) in respect to a persistent orographic rainfall that could affect an entire region, trigger diffuse terrain instabilities and reactivate also deep-seated landslides (Longoni et al., 2011; Rotunno and Houze, 2007; Tropeano, 1997). In this regard, the local rain gauges series have been integrated with the NCEP reanalysis maps data and the SLPT index was evaluated applying the theory of the Norwegian Cyclone Model. The implementation of this methodology has represented an innovative way to gain a comprehensive meteorological description of the rainfall triggers. In fact, in the NCM model, the ground-based rainfall series represent only one term (T_4) that is involved in the EC intensification. The former depends also on other processes: the upper layer divergence (T_1), boundary layer pumping (T_2) and low-pressure advection (T_3). This additional information has been addressed to play an important role in EC evolution and helped us on better differentiate critical events characteristics.

The SLPT index formulation requires several data about triggers. These can be retrieved easily by looking at a reanalysis database such as the NCEP reanalysis maps. However, NCEP maps interpretation is rather useful only for past events. Nowadays LAMs are much more suitable for interpreting the mechanism of EC through a complex orographical~~ly~~ area like the Alps (Ralph et al., 2004; Rotunno and Houze, 2007). In this regard, the NCM model is still valid but the processes involved can be interpreted at a higher detail level with LAMs, avoiding some of the hypothesis required by NCM. The evaluation of the SLPT index should be intended as propaedeutic to further analysis and it cannot be adopted in every situation. As we have foreseen from results, concerning I-D thresholds methodology, the SLPT estimation requires ~~to move~~moving from a very local perspective to a regional scale. This operation makes sense if the investigated area is rather extended for excluding very site-specific chain effects that can be triggered by isolated rainfall episodes, such as

thunderstorm cells. Another important limitation on the applicability of the SLPT index regards the presence of a recognizable EC's structure from meteorological maps. In fact, for weak EC's, the estimation of the trigger's magnitude may bring larger errors. In our study, this fact was experienced for the cases of 1953, 2008 and 2019 and was confirmed through visual inspection of NCEP maps. In these situations, the rainfall analysis should be restricted to a more local domain trying to include also LAMs outputs, radiosonde, and satellite data (Abbate et al., 2021) and the application of MI index could be much more appropriated for the magnitude estimation.

As a result of our study, we have compared the two MI and SLPT indexes to assess the magnitude of critical events. Even if they come from different theories, MI is based on frequency-magnitude theory and SLPT is has a physical meaning in the meteorology field, appears clear how they are in accordance depicting the same critical events with the highest magnitudes. This outcome has found ~~a~~ confirmation in the qualitative information we retrieved in the historical database. These results have demonstrated that exists a strong cause-effect relationship among the strength of EC developed at a regional scale in respect to the effects recorded on a local scale, especially for strong events. For the dataset examined, the SLPT comparison with the MI index was rather encouraging, $R^2 = 0.88$, and the additional information retrieved from NECP maps has sharply improved the rainfall reanalysis completeness. In our opinion, both proposed indexes are useful instruments for describing the magnitude of the rainfall-induced events, overcoming the uncertainties of the I-D threshold methodology.

6 Conclusions

This study presents an extended reanalysis of the meteorological triggering factors that have caused in the past several ~~hydrogeological~~geo-hydrological issues in the alpine mountain territory of the Sondrio Province, Northern Lombardy, Italy. Excluding the geomorphological predisposing causes of the area, the attention was pointed out to the characteristics of the rainfall. The main goal of our study was to assign a quantitative magnitude ranking to the meteorological trigger, following two approaches.

In the first one, the I-D threshold curve analysis was considered to identify critical rainfall events. We have demonstrated that the events fit some I-D thresholds, in particular the local thresholds of Cancelli-Nova and Ceriani, and that the distance from the curve does not necessarily mean that an event has a higher RP. For this reason, ~~in order~~ to assign a magnitude to each of the events, we proposed the MI index, which integrates the return period and the spatial extent of the event. The MI index was determined analytically starting from the frequency-magnitude theory, under the hypothesis that the event's magnitude was also a function of the spatial distribution of the trigger, described by the parameter AA. In the second approach, the trigger's analysis was conducted from a simply meteorological viewpoint evaluating the strength of extratropical cyclone structure through the NCM model. Using the information of NCEP reanalysis maps the SLPT index was determined and interpreted as another trigger's magnitude index, much like the MI.

The two indexes have been compared showing good accordance in the assessment of a magnitude ranking for the studied events. The SLPT index has confirmed the important relationship ~~among~~ between the EC's intensity at a regional scale and

the correspondent trigger's magnitude recorded locally, described by the MI. The two indexes are based on meteorological data ~~therefore~~, therefore, may found an application in the now-casting meteorology field. This could represent an important advancement, especially for the early warning systems adopted by municipalities for ~~hydrogeological~~geo-hydrological risks mitigation.

In view of the future climate change that, with high confidence (Faggian, 2015), will affect the Mediterranean and the Alpine environment, extreme meteorological events are supposed to increase (Ciervo et al., 2017; Gariano and Guzzetti, 2016; Moreiras et al., 2018) and also ~~hydrogeological~~geo-hydrological hazards may rise in frequency. Our study moves in this direction, trying to extend the interpretation of rainfall triggering factors through a more meteorological perspective.

Code and data availability: All the data reported in this paper are freely consultable on Internet websites. In particular, reanalysis weather maps are freely downloadable from Meteociel Website (MeteoCiel, 2020), IFFI and AVI database are freely consultable and downloadable from (Sistema Informativo sulle Catastrofi idrogeologiche; Inventario Fenomeni Franosi), and rain gauges data are extracted from local Environmental Agency (ARPA Lombardia, 2020). The model applied in this work is also freely consultable and downloadable from (Stull, 2017).

Author Contribution: Andrea Abbate and Laura Longoni conceptualized the study. Andrea Abbate carried out the formal analysis and wrote~~prepared~~ the manuscript with contributions from all co-authors. Laura Longoni and Monica Papini supervised the research and alla the authors ~~Laura Longoni~~ the reviewed & edited the manuscript~~ting~~.

Competing Interests: The authors declare that they have no conflict of interest.

Acknowledgments: The authors acknowledge the support provided by Fondazione CARIPLO through funding the project MHYCONOS, grant number 2017-0737 and to the "Geoinformatics and Earth Observation for Landslide Monitoring" project financed by "Ministero degli affari esteri e la cooperazione internazionale", in cooperation with Hanoi University of Natural Resources and Environment, Vietnam.

References

Abbate, A., Longoni, L., Ivanov, V. I., and Papini, M.: Wildfire impacts on slope stability triggering in mountain areas, 9, 1–15, https://doi.org/10.3390/geosciences9100417, 2019.

Abbate, A., Longoni, L., and Papini, M.: Extreme Rainfall over Complex Terrain: An Application of the Linear Model of Orographic Precipitation to a Case Study in the Italian Pre-Alps, MDPI Geosciences, 18, 2021.

ha formattato: Tipo di carattere: Non Grassetto

ha formattato: Inglese (Stati Uniti)

Albano, R., Mancusi, L., and Abbate, A.: Improving flood rick analysis for effectively supporting the implementation of flood risk management plans: The case study of "Serio" Valley, 75, 158–172, https://doi.org/10.1016/j.envsci.2017.05.017, 2017a.

Albano, R., Mancusi, L., and Abbate, A.: Improving flood risk analysis for effectively supporting the implementation of flood risk management plans: The case study of "Serio" Valley, Environmental Science & Policy, 75, 158–172, https://doi.org/10.1016/j.envsci.2017.05.017, 2017b.

Andrews, D. G.: An Introduction to Atmospheric Physics, Cambridge Press, Cambridge, 2010.

Rete Monitoraggio Idro-nivo-meteorologico: www.arpalombardia.it/stiti/arpalombardia/meteo.

Ballio, F., Brambilla, D., Giorgetti, E., Longoni, L., Papini, M., and Radice, A.: Evaluation of sediment yield from valley slope, 67, 149–160, https://doi.org/10.2495/DEB100131, 2010.

Bogaard, T. and Greco, R.: Invited perspectives: Hydrological perspectives on precipitation intensity-duration thresholds for landslide initiation: proposing hydro-meteorological thresholds, 18, 31–39, https://doi.org/10.5194/nhess-18-31-2018, 2018.

Bovolo, C. I. and Bathurst, J. C.: Modelling catchment-scale shallow landslide occurrence and sediment yield as a function of rainfall return period, 26, 579–596, https://doi.org/10.1002/hyp.8158, 2011.

Bovolo, C. I. and Bathurst, J. C.: Modelling catchment-scale shallow landslide occurrence and sediment yield as a function of rainfall return period, Hydrological Processes, 26, 579–596, https://doi.org/10.1002/hyp.8158, 2012.

Bronstert, A., Agarwal, A., Boessenkool, B., Crisologo, I., Peter, M., Heistermann, M., Köhn-Reich, L., López-Tarazón, J. A., Moran, T., Ozturk, U., Reinhardt-Imjela, C., and Wendi, D.: Forensic hydro-meteorological analysis of an extreme flash flood: The 2016-05-29 event in Braunsbach, SW Germany, Science of The Total Environment, 630, https://doi.org/10.1016/j.scitotenv.2018.02.241, 2018.

Caine, N.: The rainfall intensity duration control of shallow landslide and debris flow, 62, 659–675, https://doi.org/https//doi.org/10.2307/520449, 1980.

Ceriani, M., Lauzi, S., and Padovan, M.: Rainfall thresholds triggering debris-flow in the alpine area of Lombardia Region, central Alps – Italy, in: In Proceedings of the Man and Mountain'94, First International Congress for the Protection and Development of Mountain Environmen, Ponte di Legno (BS), Italy, 1994.

Ciccarese, G., Mulas, M., Alberoni, P., Truffelli, G., and Corsini, A.: Debris flows rainfall thresholds in the Apennines of Emilia-Romagna (Italy) derived by the analysis of recent severe rainstorms events and regional meteorological data, 358, 1–20, https://doi.org/10.1016/j.geomorph.2020.107097, 2020.

Ciervo, F., Rianna, G., Mercogliano, P., and Papa, M. N.: Effects of climate change on shallow landslides in a small coastal catchment in southern Italy, 14, 1043–1055, https://doi.org/10.1007/s10346-016-0743-1, 2017.

Sistema Informativo sulle Catastrofi idrogeologiche: www.db.gndci.cnr.it.

Monitoring European climate using surface observations: http://surfobs.climate.copernicus.eu/surfobs.php.

Corominas, J., van Westen, C., Frattini, P., Cascini, L., Malet, J.-P., Fotopoulou, S., Catani, F., Van Den Eeckhaut, M., Mavrouli, O., Agliardi, F., Pitilakis, K., Winter, M. G., Pastor, M., Ferlisi, S., Tofani, V., Hervás, J., and Smith, J. T.:

Recommendations for the quantitative analysis of landslide risk, Bulletin of Engineering Geology and the Environment, 73, 209–263, https://doi.org/10.1007/s10064-013-0538-8, 2014.

Crosta, G. and Frattini, P.: Rainfall thresholds for triggering soil slips and debris flow, Proceedings of the 2nd EGS Plinius Conference on Mediterranean Storms, 463–487, 2001.

De Michele, C., Rosso, R., and Rulli, M. C.: Il Regime delle Precipitazioni Intense sul Territorio della Lombardia: Modello di Previsione Statistica delle Precipitazioni di Forte Intensità e Breve Durata, ARPA Lombardia, Milano, 2005.

Faggian, P.: Climate change projection for Mediterranean Region with focus over Alpine region and Italy, 4, 482–500, https://dori.org/10.17265/2162-5263/2015.09.004, 2015.

Frattini, P., Crosta, G., and Sosio, R.: Approaches for defining thresholds and return periods for rainfall-triggered shallow landslides, Hydrological Processes, 23, 1444–1460, https://doi.org/10.1002/hyp.7269, 2009.

Gao, L., Zhang, L. M., and Cheung, R. W. M.: Relationships between natural terrain landslide magnitudes and triggering rainfall based on a large landslide inventory in Hong Kong, Landslides, 15, 727–740, https://doi.org/10.1007/s10346-017-0904-x, 2018.

Gao, Y., Chen, N., Hu, G., and Deng, M.: Magnitude-frequency relationship of debris flows in the Jiangjia Gully, China, Journal of Mountain Science, 16, 1289–1299, https://doi.org/10.1007/s11629-018-4877-6, 2019.

Gariano, S. L. and Guzzetti, F.: Landslides in a changing climate, Earth-Science Reviews, 162, 227–252, https://doi.org/10.1016/j.earscirev.2016.08.011, 2016.

Godson, W. L.: A new tendency equation and its application to the analysis of surface pressure changes, 5, 227–235, 1948.

Grazzini, F.: Predictability of a large-scale flow conducive to extreme precipitation over the western Alps, Meteorology and Atmospheric Physics, 95, 123–138, https://doi.org/10.1007/s00703-006-0205-8, 2007.

Grazzini, F. and Vitart, F.: Atmospheric predictability and Rossby wave packets, Quarterly Journal of the Royal Meteorological Society, 141, 2793–2802, https://doi.org/10.1002/qj.2564, 2015.

Gutenberg, B. and Richter, C. F.: Frequency of earthquakes in California*, Bulletin of the Seismological Society of America, 34, 185–188, 1944.

Guzzetti, F., Reichenbach, P., Cardinali, M., Galli, M., and Ardizzone, F.: Probabilistic landslide hazard assessment at the basin scale, Geomorphology, 72, 272–299, https://doi.org/10.1016/j.geomorph.2005.06.002, 2005.

Guzzetti, F., Peruccacci, S., Rossi, M., and Stark, C. P.: Rainfall thresholds for the initiation of landslides in central and southern Europe, Meteorology and Atmospheric Physics, 98, 239–267, https://doi.org/10.1007/s00703-007-0262-7, 2007.

Guzzetti, F., Peruccacci, S., Rossi, M., and Stark, C. P.: The rainfall intensity–duration control of shallow landslides and debris flows: an update, Landslides, 5, 3–17, https://doi.org/10.1007/s10346-007-0112-1, 2008.

Ibsen, M.-L. and Casagli, N.: Rainfall patterns and related landslide incidence in the Porretta-Vergato region, Italy, Landslides, 1, 143–150, https://doi.org/10.1007/s10346-004-0018-0, 2004.

Iida, T.: Theoretical research on the relationship between return period of rainfall and shallow landslides, Hydrological Processes, 18, 739–756, https://doi.org/10.1002/hyp.1264, 2004.

ha formattato: Italiano (Italia)

Inventario Fenomeni Franosi: http://www.isprambiente.gov.it/it/progetti/suolo-e-territorio-1/iffi-inventario-dei-fenomeni-franosi-in-italia.

ISPRA: Dissesto idrogeologico in Italia: pericolosità e indicatori di rischio, ISPRA, Ispra, 2018.

SCIA: Sistema Nazionale per l'elaborazione e diffusione di dati climatici: http://www.scia.isprambiente.it.

Iverson, R. M.: Landslide triggering by rain infiltration, Water Resources Research, 36, 1897–1910, https://doi.org/10.1029/2000WR900090, 2000.

Jie, T., Zhang, B., He, C., and Yang, L.: Variability In Soil Hydraulic Conductivity And Soil Hydrological Response Under Different Land Covers In The Mountainous Area Of The Heihe River Watershed, Northwest China, Land Degradation & Development, 28, https://doi.org/10.1002/ldr.2665, 2016.

Kalnay, E., Kanamitsu, M., Kistler, R., Collins, W., Deaven, D., Gandin, L., Iredell, M., Saha, S., White, G., Woollen, J., Zhu, Y., Chelliah, M., Ebisuzaki, W., Higgins, W., Janowiak, J., Mo, K. C., Ropelewski, C., Wang, J., Leetmaa, A., Reynolds, R., Jenne, R., and Joseph, D.: The NCEP/NCAR 40-Year Reanalysis Project, Bull. Amer. Meteor. Soc., 77, 437–472, https://doi.org/10.1175/1520-0477(1996)077<0437:TNYRP>2.0.CO;2, 1996.

Kim, S. W., Chun, K. W., Kim, M., Catani, F., Choi, B., and Seo, J. I.: Effect of antecedent rainfall conditions and their variations on shallow landslide-triggering rainfall thresholds in South Korea, Landslides, https://doi.org/10.1007/s10346-020-01505-4, 2020.

Lazzari, M., Piccarreta, M., and Manfreda, S.: The role of antecedent soil moisture conditions on rainfall-triggered shallow landslides, 2018, 1–11, https://doi.org/10.5194/nhess-2018-371, 2018.

Longoni, L., Papini, M., Arosio, D., and Zanzi, L.: On the definition of rainfall thresholds for diffuse landslides, 53, 27–41, https://doi.org/10.2495/978-1-84564-650-9/03, 2011.

Longoni, L., Papini, M., Arosio, D., Zanzi, L., and Brambilla, D.: A new geological model for Spriana landslide, Bulletin of Engineering Geology and the Environment, 73, 959–970, https://doi.org/10.1007/s10064-014-0610-z, 2014.

Longoni, L., Ivanov, V. I., Brambilla, D., Radice, A., and Papini, M.: Analysis of the temporal and spatial scales of soil erosion and transport in a Mountain Basin, 16, 17–30, https://doi.org/10.4408/IJEGE.2016-02.O-02, 2016.

Malamud, B. D., Turcotte, D. L., Guzzetti, F., and Reichenbach, P.: Landslide inventories and their statistical properties, Earth Surface Processes and Landforms, 29, 687–711, https://doi.org/10.1002/esp.1064, 2004.

Martin, J. E.: Mid-Latitude Atmosphere Dynamics, Wiley, Chichester, West Sussex, England, 2006.

Observations, Prévisions, Modèles en temps réel: www.meteociel.fr.

Montrasio, L.: Stability of soil-slip, 45, 357–366, https://doi.org/10.2495/RISK000331, 2000.

Montrasio, L. and Valentino, R.: Modelling Rainfall-induced Shallow Landslides at Different Scales Using SLIP - Part II, Procedia Engineering, 158, 482–486, https://doi.org/10.1016/j.proeng.2016.08.476, 2016.

Moreiras, S., Vergara Dal Pont, I., and Araneo, D.: Were merely storm-landslides driven by the 2015-2016 Niño in the Mendoza River valley?, Landslides, 15, https://doi.org/10.1007/s10346-018-0959-3, 2018.

ha formattato: Italiano (Italia)

National Center for Environmental Information: https://www.ncei.noaa.gov/.

Olivares, L., Damiano, E., Mercogliano, P., Picarelli, L., Netti, N., Schiano, P., Savastano, V., Cotroneo, F., and Manzi, M. P.: A simulation chain for early prediction of rainfall-induced landslides, Landslides, 11, 765–777, https://doi.org/10.1007/s10346-013-0430-4, 2014.

Ozturk, U., Tarakegn, Y., Longoni, L., Brambilla, D., Papini, M., and Jensen, J.: A simplified early-warning system for imminent landslide prediction based on failure index fragility curves developed through numerical analysis, Geomatics, Natural Hazards and Risk, https://doi.org/10.1080/19475705.2015.1058863, 2015.

Ozturk, U., Wendi, D., Crisologo, I., Riemer, A., Agarwal, A., Vogel, K., López-Tarazón, J. A., and Korup, O.: Rare flash floods and debris flows in southern Germany, Science of The Total Environment, 626, https://doi.org/10.1016/j.scitotenv.2018.01.172, 2018.

Papini, M., Ivanov, V., Brambilla, D., Arosio, D., and Longoni, L.: Monitoring bedload sediment transport in a pre-Alpine river: An experimental method, Rendiconti Online della Società Geologica Italiana, 43, 57–63, https://doi.org/10.3301/ROL.2017.35, 2017.

Peres, D. J., Cancelliere, A., Greco, R., and Bogaard, T. A.: Influence of uncertain identification of triggering rainfall on the assessment of landslide early warning thresholds, 18, 633–646, https://doi.org/10.5194/nhess-18-633-2018, 2018.

Peruccacci, S., Brunetti, M. T., Gariano, S. L., Melillo, M., Rossi, M., and Guzzetti, F.: Rainfall thresholds for possible landslide occurrence in Italy, Geomorphology, 290, 39–57, https://doi.org/10.1016/j.geomorph.2017.03.031, 2017.

Piciullo, L., Gariano, S. L., Melillo, M., Brunetti, M. T., Peruccacci, S., Guzzetti, F., and Calvello, M.: Definition and performance of a threshold-based regional early warning model for rainfall-induced landslides, Landslides, 14, 995–1008, https://doi.org/10.1007/s10346-016-0750-2, 2017.

Ralph, F. M., Neiman, P. J., and Wick, G. A.: Satellite and CALJET Aircraft Observations of Atmospheric Rivers over the Eastern North Pacific Ocean during the Winter of 1997/98, Monthly Weather Review, 132, 1721–1745, https://doi.org/10.1175/1520-0493(2004)132<1721:SACAOO>2.0.CO;2, 2004.

Rappelli, F.: Definizione delle soglie pluviometriche d'innesco frane superficiali e colate torrentizie: accorpamento per aree omogenee, IRER, Istituto Regionale di Ricerca della Lombardia, Milano, 2008.

Reid, L. and Page, M. J.: Magnitude and frequency of landsliding in a large New Zealand catchment, Geomorphology, 49, 71–88, https://doi.org/10.1016/S0169-555X(02)00164-2, 2003.

Ronchetti, F., Borgatti, L., Cervi, F., C, G., Piccinini, L., Vincenzi, V., and Alessandro, C.: Groundwater processes in a complex landslide, northern Apennines, Italy, Natural Hazards and Earth System Sciences, 9, 895–904, https://doi.org/10.5194/nhess-9-895-2009, 2009.

Rosi, A., Peternel, T., Jemec-Auflič, M., Komac, M., Segoni, S., and Casagli, N.: Rainfall thresholds for rainfall-induced landslides in Slovenia, Landslides, 13, 1571–1577, https://doi.org/10.1007/s10346-016-0733-3, 2016.

Rossi, M., Peruccacci, S., Brunetti, M., Marchesini, I., Luciani, S., Ardizzone, F., Balducci, V., Bianchi, C., Cardinali, M., Fiorucci, F., Mondini, A., Paola, R., Salvati, P., Santangelo, M., Bartolini, D., Gariano, S. L., Palladino, M., Vessia, G., Viero, A., and Tonelli, G.: SANF: National warning system for rainfall-induced landslides in Italy, https://doi.org/10.13140/2.1.4857.9527, 2012.

ha formattato: Italiano (Italia)

ha formattato: Italiano (Italia)

ha formattato: Italiano (Italia)

Rossi, M., Guzzetti, F., Salvati, P., Donnini, M., Napolitano, E., and Bianchi, C.: A predictive model of societal landslide risk in Italy, Earth-Science Reviews, 196, 102849, https://doi.org/10.1016/j.earscirev.2019.04.021, 2019.

Rosso, R., Rulli, M. C., and Vannucchi, G.: A physically based model for the hydrologic control on shallow landsliding, Water Resour. Res, 42, https://doi.org/10.1029/2005WR004369, 2006.

Rotunno, R. and Houze, R.: Lessons on orographic precipitation for the Mesoscale Alpine Programme, Quarterly Journal of the Royal Meteorological Society, 133, 811–830, https://doi.org/10.1002/qj.67, 2007.

Sanders, F. and Gyakum, J. R.: Synoptic-Dynamic Climatology of the "Bomb," Mon. Wea. Rev., 108, 1589–1606, https://doi.org/10.1175/1520-0493(1980)108<1589:SDCOT>2.0.CO;2, 1980.

Segoni, S., Rossi, G., Rosi, A., and Catani, F.: Landslides triggered by rainfall: A semi-automated procedure to define consistent intensity–duration thresholds, Computers & Geosciences, 63, 123–131, https://doi.org/10.1016/j.cageo.2013.10.009, 2014.

Stull, R. B.: Practical Meteorology: An Algebra-based Survey of Atmospheric Science., University of British Columbia, Vancouver, Canada, 2017.

Tropeano, D.: Inondazioni e frane in Lombardia: un problema storico, in: Utilizzo dei dati storici per la determinazione delle aree esondabili nelle zone alpine, CNR-IRPI, Torino, 47–109, 1997.

Vessia, G., Parise, M., Brunetti, M. T., Peruccacci, S., Rossi, M., Vennari, C., and Guzzetti, F.: Automated reconstruction of rainfall events responsible for shallow landslides, 14, 2399–2408, https://doi.org/10.5194/nhess-14-2399-2014, 2014.

Vessia, G., Pisano, L., Vennari, C., Rossi, M., and Parise, M.: Mimic expert judgement through automated procedure for selecting rainfall events responsible for shallow landslide: A statistical approach to validation, Computers & Geosciences, 86, 146–153, https://doi.org/10.1016/j.cageo.2015.10.015, 2016.

Wallace, J. M. and Hobbs, P. V.: Atmospheric Science: an introductory survey, Elsevier, Oxford, 2006.

Xiao, L., Wang, J., Zhu, Y., and Zhang, J.: Quantitative Risk Analysis of a Rainfall-Induced Complex Landslide in Wanzhou County, Three Gorges Reservoir, China, International Journal of Disaster Risk Science, 11, 347–363, https://doi.org/10.1007/s13753-020-00257-y, 2020.

Fig. 11: The logo of Copernicus Publications.

ha formattato: Italiano (Italia)

OLD VERSION MANUSCRIPT

Meteorology triggering factors analysis for rainfall induced hydrogeologicalgeo-hydrological events in alpine region

Andrea Abbate[1], Monica Papini[1], Laura Longoni[1]
[1] Department of Civil Engineering (DICA), Politecnico di Milano, Milano 20133, Italy
Correspondence to: Laura Longoni (laura.longoni@polimi.it)

Abstract. This paper presents an extended back analysis of the major hydrogeologicalgeo-hydrological events that occurred in the last 70 years in the alpine area of the Lombardy region, Italy. This work is focused on the description and the interpretation of the major meteorological triggering factors that have caused these mass movements.

ha formattato: Inglese (Stati Uniti)

The triggering factors for each hydrogeologicalgeo-hydrological event were analysed into twofold approaches, with the final intent of ranking their magnitude in terms of consequent damages. Firstly, an analysis of precipitation was conducted using local rain-gauge data, comparing them against rainfall threshold curves proposed by several authors. Moreover, the return time of precipitation and the information about the spatial extension of the triggering factors were considered for the assessment of an empirical magnitude index of the hydrogeologicalgeo-hydrological event. Secondly, considering the currently available meteorological reanalysis database, provided globally by National Centres of Environmental Prediction (NCEP), additional information on the dynamics, the nature and intensity of meteorological triggers were taken into account. The two approaches were compared throughout two indexes that tried to assess the strength of rainfall phenomena: the first one is empirical while the second one is physical.

The results obtained from the application of the two methodologies have been discussed. The rainfall method permits to highlight which are the critical hydrogeologicalgeo-hydrological events, not giving any quantitative information about their magnitude. The second approach analyses better the characteristic and the dynamic of meteorological triggers, suggesting, through a physical index, a quantitative ranking of their intensities that has revealed to be a good predictor for the magnitude of hydrogeologicalgeo-hydrological rainfall-induced events.

1 Introduction

Landslides represent one of the main hydrogeologicalgeo-hydrological hazards in Alpine and Apennines regions (Albano et al., 2017; Ballio et al., 2010; Caine, 1980; Gao et al., 2018). Italy is a country historically affected by a diffuse hydrogeologicalgeo-hydrological fragility of the environment (Longoni et al., 2016) and mountain slopes are the most vulnerable places where landslides and flash floods can occur (Iverson, 2000; Longoni et al., 2011; Montrasio, 2000; Montrasio and Valentino, 2016). This is the case of Valtellina (Lombardy) in 1987 as well as Piedmont in 1994 and 2000 and Genova city in 2011 and 2013, which were affected by several flash floods and landslides phenomena. All of these catastrophic events have been caused by exceptional meteorological events that rarely occur and have particular features regards their duration and their intensity (Ceriani et al., 1994).

In the context of hydrogeologicalgeo-hydrological risk prevention, urban planners and infrastructure engineers have to deal with the analysis of triggering factors and need instruments for its quantification (Ozturk et al., 2015; Papini et al., 2017; Piciullo et al., 2017; Rossi et al., 2019). In this paper, a back analysis of the meteorological triggers of past hydrogeologicalgeo-hydrological events is presented. Indeed, a quantitative study of local precipitation is mandatory to correlate these meteorological events with landslide failures (Corominas et al., 2014; Guzzetti et al., 2007).

A common approach used consists of the analysis of the return period (RP) of the triggering rainfall (Caine, 1980; Iverson, 2000). It is not trivial to evaluate the recurrence of a flood or a landslide unless we make a hypothesis of iso-frequency with the RP of precipitation (De Michele et al., 2005; ISPRA, 2018). For a flood that occurred in a flood plain or in a large valley, this hypothesis is generally acceptable due to the fact that it can happen even though a large amount of water is available,

Codice campo modificato

Codice campo modificato

~~coming from an intense and prolonged meteorological event (Albano et al., 2017; De Michele et al., 2005). For a landslide failure, defining a return period is not a common practice because it is not a periodic event but a sudden collapse (ISPRA, 2018). This is particularly true for complex and deep landslide where the triggering factors are intimately bounded with the local predisposing factors, i.e. the territory morphology, geology, etc. (Ciccarese et al., 2020; Guzzetti et al., 2007; ISPRA, 2014, 2018; Longoni et al., 2016; Montrasio, 2000; Ozturk et al., 2015; Papini et al., 2017). Therefore, try to interpret this cause-effect relationship looking only at the rainfall series cannot be used.~~

~~However, for shallow landslides and debris flows hazard assessment, are considered the rainfall intensity-duration curves (Ceriani et al., 1994; Ciccarese et al., 2020; Gao et al., 2018; Longoni et al., 2011; Olivares et al., 2014; Rappelli, 2008; Rosi et al., 2016; Rossi et al., 2019). These define a rainfall threshold for a specific region on which, taking into account the duration and the average intensity of the rainfall episode, a landslide could be triggered. This interpretation is acceptable, considering this type of landslide rainfall-induced (Ceriani et al., 1994; Guzzetti et al., 2007; Piciullo et al., 2017; Rosi et al., 2016). These thresholds data are calibrated looking at the past events occurred in the area and directly correlated with the nearest rain gauge measures (Rappelli, 2008). Intrinsically they include the susceptibility of the local territory to landslide failure so their usability generally can't be extended to other regions (Caine, 1980; Guzzetti et al., 2007; ISPRA, 2018; Longoni et al., 2011). On the other hand, this method is widely used for predicting the occurrence of shallow landslide and debris flow events but, due to its empirical nature, it is rather approximate and leads sometimes to "false alarm" detecting (Abbate et al., 2019; Guzzetti et al., 2007; Peres et al., 2018).~~

~~Even though the rainfall return period estimation and rainfall thresholds have been widely used in different parts of the world (Gao et al., 2018), some open questions still exist. Are these approaches sufficient for a complete description of triggering factors? Can rainfall analysis be improved considering also other meteorological variables, which could better describe the rainfall events and the linked consequences?~~

~~Generally, a local study on the triggering causes is not completely descriptive of the real magnitude of the meteorological triggering event (COPERNICUS, 2020; Rotunno and Houze, 2007; Stull, 2017). This is particularly true in mountain areas where the territory enhances the heterogeneity of rainfall field that is not able to exhaustively represented only taking into account the local rain gauge network (Rotunno and Houze, 2007). In particular, the type of rainfall events cannot always be recognized directly from rain gauge time-series so that other meteorological variables should be taken into account for its description. This is crucial because different precipitation type can affect the characteristics of the hydrogeological~~geo-hydrological ~~failures (Corominas et al., 2014; Guzzetti et al., 2007). An intense but rather localized rainfall, such as a thunderstorm, could trigger a certain type of hydrogeological~~geo-hydrological ~~issues, such as shallow landslides and soils slips (Montrasio, 2000). On the other hand, a persistent orographic rainfall, which could affect an entire region for several days, may have completely different effects on the territory, enhancing its hydrogeological~~geo-hydrological ~~fragility (Longoni et al., 2011; Rotunno and Houze, 2007; Tropeano, 1997). Therefore, a more complete description of the type of triggering factor is necessary to better explain the territorial hydrogeological~~geo-hydrological ~~dynamics.~~

Codice campo modificato

Codice campo modificato

Codice campo modificato

The goal of this paper is to investigate the relationship between hydrogeologicalgeo-hydrological issues and their triggering factors in a broader sense, starting from the back analysis of past hydrogeologicalgeo-hydrological events, where landslide and flash flood occurred. The alpine region in the northern part of Lombardy, Italy, was considered because of its past critical hydrogeologicalgeo-hydrological events (CNR, 2020; ISPRA, 2014; Rappelli, 2008; Tropeano, 1997). Triggering factors were analysed into twofold approaches. The first one uses only local rainfall data applying the threshold curves method as a reference for detecting shallow landslide failure. The second considers also meteorological reanalysis maps provided globally by National Centres of Environmental Prediction (NCEP) (Kalnay et al., 1996; MeteoCiel, 2020; NOAA, 2020) where is possible to gather additional information about the spatial and temporal evolution of the triggering events at larger scale (Andrews, 2010; Grazzini, 2007; Grazzini and Vitart, 2015; Stull, 2017).

The paper will be organized as follows: in section 2 is presented the databases of the historical hydrological events and the materials and methods adopted in our analysis of triggering factors related to these events. In section 3 the results and relative discussion are reported, with some comparisons and comments regarding the two approaches and in section 4 some final remarks and conclusions of the ongoing research work are reported.

2 Data, Methods and Models

This section presents the methodology followed for the back analysis.

2.1 Historical database of hydrogeologicalgeo-hydrological events

A group of past hydrogeologicalgeo-hydrological events has been considered for the alpine area of Sondrio Province, northern Lombardy, Italy, Figure 1. This area was affected by exceptional hydrogeologicalgeo-hydrological events in July 1987 causing extended damages and loss of lives (CNR, 2020). The most important and severe was the Val Pola landslide that occurred in the upper part of Valtellina and happened as a sudden collapse of 40 million cubic meter of old debris, destroying 5 villages and six hamlets with 35 people died of various disaster-related causes (Tropeano, 1997). On the other hand, the entire province was also affected mainly by diffuse hydrogeologicalgeo-hydrological episodes such as shallow landslide and flash floods, that caused people injuries and comparable damages to infrastructure and buildings, estimated in 2 billion of euros. These hydrogeologicalgeo-hydrological issues were caused by a rather intense and prolonged rainfall episode (Rappelli, 2008; Tropeano, 1997) and the effects were enhanced by rapid glacier melting increased by high-altitude summer temperatures.

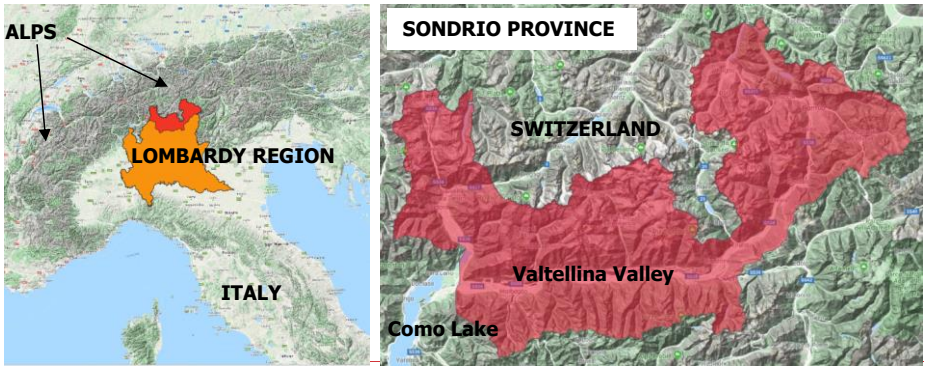

Figure 1: Case Study Area of Sondrio province, northern Lombardy, base layer from © Google Maps 2020.

The back analysis has considered also other critical hydrogeologicalgeo-hydrological episodes like the 1987 that affected the Sondrio Province. Two different data sources have been used to collect data for the analysis of the historical hydrogeologicalgeo-hydrological events: the "Aree Vulnerate Italiane" (AVI) database and the "Inventario Fenomeni Franosi Italiano" (IFFI) database (CNR, 2020; ISPRA, 2014). The AVI database is directly available inside a geoportal web site that is managed by CNR (Centro Nazionale della Ricerca) and the IFFI database, available from the national geoportal website (CNR, 2020; ISPRA, 2014). The data stored collects historical information from past natural disaster starting from the medieval age up to nowadays. Looking at the available time-series, data are not homogeneous and the lack of information is generally diffused (CNR, 2020; ISPRA, 2018). For the area of Sondrio Province, a quite extensive historical bibliography was found in literature (Ceriani et al., 1994) that considers all the events starting from 1850 up to 2000. In this case, the two databases' consistency was evaluated, and redundant records have been corrected. Then, a merging operation between the AVI and the IFFI database information was needed for the years comprised between 2000 and 2019.

The period chosen for the back analysis is comprised between 1951 and 2019. Indeed, systematic monitoring of the precipitation and temperature started in Italy since 1951 by SIMN (Servizio Idrografico e Mareografico Nazionale) and looking at the antecedent periods these data were missed or characterized by several uncertainties or errors (ISPRA, 2019).

The available rain gauge data series were gathered from local archives of SIMN (ISPRA, 2019) and ARPA Lombardia (Agenzia Nazionale per la Protezione dell'Ambiente) (ARPA Lombardia, 2020). These series have been conventionally recorded on daily bases until the 2000s years so "a daily rain" represents the maximum resolution of our dataset before that period. Starting from 2001, the increased temporal resolution available that moved to a sub-hourly time-step increased the accuracy of the rainfall analysis.

The list of the hydrogeologicalgeo-hydrological events analysed in the study and their description retrieved from AVI and IFFI databases is reported in Table 1.

Codice campo modificato

Codice campo modificato

Table 1: HydrogeologicalGeo-hydrological events recorded from 1951 up to 2019 considered for the back-analysis study. In the table are reported the starting and ending date for each event, the typology of the meteorological triggers, the hydrogeologicalgeo-hydrological effects on the territory, the information about the extension of the territorial area affected [km^2], the extreme localized events (EXL) and the more diffuse ones (DIF), the cumulated rain [mm] gathered by local rain gauges and the event duration [days].

YEAR	START	FINISH	METEO TYPE	EFFECTS	EXTENSION TYPE	ESTIMATED AFFECTED AREA [km^2]	CUMULATED RAIN [mm]	EVENT DURATION [days]
1951	7 august	8 august	Heavy rainfall	Flash Floods	EXL	500	218	2.0
1953	17 july	18 july	Heavy rainfall	Flash Floods	EXL	125	83.8	1.0
1960	15 september	17 september	Heavy rainfalls	Landslide and Floods	DIF	2000	115.6	2.0
1966	3 november	5 november	Prolonged rainfalls	Landslides and Floods	DIF	3000	128.6	3.0
1983	21 may	23 may	Heavy rainfalls	Landslides	EXL	100	208.6	3.0
1987	16 july	19 july	Prolonged rainfalls	Landslides and Floods	DIF	4000	254.8	3.0
1997	26 june	29 june	Prolonged rainfalls	Landslides and Floods	EXL	200	275	3.0
2000	13 november	17 november	Prolonged rainfalls	Landslides	DIF	2000	218.7	4.0
2002	13 november	18 november	Prolonged rainfalls	Landslides	DIF	3000	308.8	5.0
2008	12 july	13 july	Heavy rainfalls	Landslides	EXL	240	60	0.5
2018	27 october	30 october	Prolonged rainfalls	Landslides	DIF	3000	242.4	3.6
2019	11 june	12 june	Heavy rainfall	Landslides and Floods	EXL	700	150	0.7

The precise location of each hydrogeologicalgeo-hydrological event was not directly reported in the dataset, but an indication of the municipalities affected by hydrogeologicalgeo-hydrological issues was present. These data were taken into consideration for defining the extension of the triggering phenomena and were corrected looking at the recorded rain gauges series. In particular, rainfall events were distinguished in two types: extremely localized events (EXL), with an influence area lower than 1000 km^2, or diffuse events (DIF), with significant territorial diffusion greater than 1000 km^2. This value has been motivated considering the nature of the meteorological triggers: "EXL" were generally associated with convective rainfall phenomena which extension has an order of 10 x 10 km^2 and "DIF" were characterized by diffuse and uniform rainfall with an extension around 100 x100 km^2(Martin, 2006; Rotunno and Houze, 2007).

The dataset analysis of Table 1 shows a clear seasonal distribution of the events mainly concentrated during summer and autumn. July and November are the months much more prone to hydrogeologicalgeo-hydrological events and this strong seasonality highlights that triggers phenomena involved may have a different nature (Martin, 2006; Rotunno and Houze, 2007). In July, meteorological events are characterized mainly by high intensity and short duration with a typical convective behaviour of precipitation (thunderstorms), and their average duration is generally around 1 or 2 days. In particular, 1951, 1953, 1987 and 2008 events happened during the summer season and rainfall cumulated were comprised between 100-200

mm, apart from 1987 and 1997 that were rather exceptional (254 mm and 275 mm in three days). During October and November, rainfall events are characterized by higher persistency (4-5 days) and rainfall cumulated can easily reach amounts around 250-350 mm, such as for the events that happened in 2000, 2002 and 2018. They are usually associated with extratropical cyclone structures that moving eastward from Atlantic Ocean can affect directly the Alpine mountain range (Martin, 2006).

These observations from the dataset have been studied in deep from a quantitative viewpoint considering the two approaches proposed: the traditional rainfall approach and the meteorological reanalysis approach.

2.2 Traditional Approach: Rainfall Threshold Curves and Rainfall Return Period analysis

The rainfall data were elaborated considering the spatial extension of the triggering events, i.e. rainfall field characteristics. For the "EXL" data, the nearest rain gauge or at least the 2 nearest rain gauges were chosen as local rainfall data. For the "DIF" group, all the available daily rain data RR_i in the affected territory have been considered and averaged with respect to the number of rain gauges stations "n" in order to obtain a representative value for RR.

$$RR = \frac{\sum_{i=1}^{n} RRi}{n} \quad (1)$$

Then, the average daily rainfall rate RR was calculated dividing the cumulative rainfall by the duration D. The results were then plotted against the local rainfall intensity-duration threshold curve. For the examined area was considered a group of threshold curves proposed in the literature by several authors.

The "Caine" curve (Caine, 1980) is the general one, valid for shallow hydrogeologicalgeo-hydrological processes around the world, Eq. (2.a). The "Ceriani" curve (Ceriani et al., 1994) was proposed in 1994 and was calibrated directly on the recorded data available in Sondrio Province, Eq. (2.b). A more recent study conducted by (Guzzetti et al., 2007) has proposed a new set of rainfall threshold curves valid for central and southern Europe, considering a distinction among different climate types. In our study, three of them have been selected: the general one Eq. (2.c), the curve valid for mid-climate Eq. (2.d) and the one suitable for highlands Eq. (2.e). All the rainfall threshold curves have a monomial expression where the D is the duration of the rainfall [hours], and the I is the average rainfall intensity [mm/h].

$$I = 14.84\, D^{-0.39} \quad (2.a)$$

$$I = 20.01\, D^{-0.55} \quad (2.b)$$

$$I = 8.67\, D^{-0.61} \quad (2.c)$$

$$I = 18.6\, D^{-0.81} \quad (2.d)$$

$$I = 8.53\, D^{-0.64} \quad (2.e)$$

A further step on rainfall analysis dealt with the evaluation of the correspondent return period (RP). The RP is directly associated with the intensity of the rainfall because it expresses the probability of recurrence of a particular rainfall event on a location (Corominas et al., 2014; De Michele et al., 2005). Using the Curve of Pluviometric Possibility (CPP) (De Michele et al., 2005) available for the Lombardy region and provided by (ARPA Lombardia, 2020), the RP of precipitation was

estimated for each event. Localized events "EXL" were treated separately with respect to the diffuse "DIF" ones. For the localized events, the on-site coefficient of CPPs has been used but for the diffusive ones, a spatially averaged value of the coefficients has been elaborated for the area of interest.

2.3 Reanalysis Approach: NCEP Reanalysis Maps

To improve the analysis of triggering factors, the database was studied considering other variables associated with the meteorological event. In particular, the National Centre for Environmental Prediction (NCEP) data (Kalnay et al., 1996; MeteoCiel, 2020) were examined. The NCEP reanalysis maps are a valuable instrument for investigating the past evolution of meteorology around a target area (Faggian, 2015; Grazzini, 2007; Rotunno and Houze, 2007; Stull, 2017). They have a spatial resolution of 2.5° x 2.5° degrees of latitude and longitude, covering the whole planet with a temporal frequency of 12 h. These maps contain information about temperature and pressure distribution at different geopotential heights, i.e. 850 hPa and 500 hPa, to describe air mass advection and front formations. The pressure values reported at sea level are valid indicators of a cyclone or anticyclone structure developments at regional scale (Andrews, 2010; Grazzini and Vitart, 2015; Stull, 2017). Moreover, the wind fluxes velocities are important for establishing the spatial and temporal evolution of a particular rainfall event (Andrews, 2010; Grazzini, 2007; Stull, 2017).

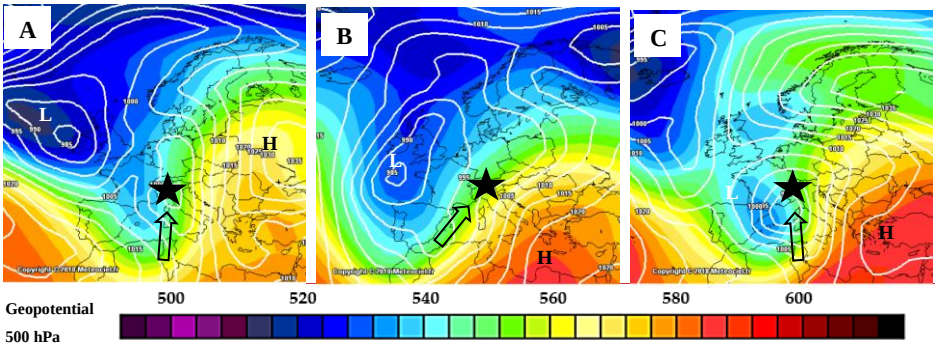

Figure 2: Reanalysis maps from NCEP reporting the Sea-Level Pressure and 500 hPa Pressure (colours) for 1966 (A), 2002 (B) and 2018 (C) events where the black star is the Sondrio Province position, adapted from (MeteoCiel, 2020), modified after.

A qualitative looking at the reanalysis maps for each considered event highlights some similarities regarding the meteorological configuration of air masses. Not surprisingly, the major hydrogeologicalgeo-hydrological events have occurred during strong extratropical cyclone (EC), as described in Figure 2.

ECs are important meteorological phenomena that develop in the Atlantic Ocean near the British Islands and are moved eastward through the Mediterranean area thanks to the dynamic of the Rossby waves at planetary scale (Grazzini and Vitart, 2015; Martin, 2006). These generate at the boundary of the polar vortex strong jet streams that can move air masses in the

direction of the southern Alps, as is represented in Figure 2. Across the southern flank of Alps, one of the critical consequences of this configuration is the enhancement of persistent and heavy orographic precipitation (Rotunno and Houze, 2007) thanks to the instauration of a strong southern moist and warm flow, the "Scirocco" wind, as reported by (Grazzini, 2007). Rainfall intensities can reach remarkably high amounts if these conditions are prolonged for several days, leading up to 400 mm in 2/3 days (Grazzini, 2007; Rotunno and Houze, 2007). In addition, the presence of convection especially during the summer season may add another level of complexity, producing a further enhancing of local rainfall rates (De Michele et al., 2005; Rotunno and Houze, 2007).

This dynamic is characterized by some peculiarities that are necessary to be understood for interpreting the local scale rainfall effects on the territory. Therefore, using the NCEP maps, a synthetic model proposed by (Godson, 1948; Martin, 2006; Stull, 2017) was chosen for the estimation of a strength index related to the extratropical cyclone intensity. The model calculates indirectly the Sea-Level Pressure Tendency (SLPT), the time-variation ratio of sea-level atmospheric pressure $\Delta p_{sl}/\Delta t$ [hPa/h], that represents an indicator of the strength of a cyclone structure (Andrews, 2010; Godson, 1948; Martin, 2006; Stull, 2017; Wallace and Hobbs, 2006). In general, this ratio is higher, in an absolute sense, when the EC is more intense. According to (Stull, 2017), this index is obtained as a sum of three different influencing factors that correspond to the most important processes implicated in the dynamic evolution of extratropical cyclone:

$$\frac{\Delta p_{sl}}{\Delta t} = T_1 + T_2 + T_3 \quad (4)$$

- T_1 expresses the "upper-level air divergence" due to jet streams, which remove air mass from an ideal atmosphere air column. W_{MID} $[m/s]$ is the mean air column vertical velocity, evaluated considering the continuity equation in the proximity of the local change of jet stream velocity gradient. $\rho_{MID} = 0.5\ kg/m^3$ is the average density of air column and $g = 9.8\ [m/s^2]$.

$$T_1 = -g\,\rho_{MID}\,W_{MID} \quad (4.a)$$

- T_2 is the "atmosphere boundary layer pumping", that causes the horizontal wind to spiral inward toward a low-pressure center. The air density of the boundary layer is $\rho_{BL} = 1.112\ kg/m^3$, $g = 9.8\ [m/s^2]$ and W_{BL} is the vertical velocities at boundary layer calculated using the approximation proposed by (Stull, 2017) for cyclone structures.

$$T_2 = g\,\rho_{BL}\,W_{BL} \quad (4.b)$$

- T_3 is the "latent heating" due to water vapor condensation in rainfall. It comes from the theory of thermodynamic transformations of water vapor in the atmosphere where all the parameters for rain condensation processes are stored in the term $b = 0.082\ [kPa/mm]$ and $RR\ [mm/h]$ is the average hourly rainfall rate. In the model proposed, the information related to the local rainfall intensity is considered only in this term while the other is in the function of the meteorological parameters retrieved from NCEP reanalysis maps [27].

$$T_3 = -b\,RR \quad (4.c)$$

When the balance in Eq. (4) is negative the cyclogenesis occurs. Indeed, the term T1 and T3 have a negative contribution and during the cyclone formation (cyclogenesis) participate in the decreasing of the SLPT index. Figure 3 reports how the model works, considering the contribution of each four components across the timeline (A to G) during the phase of EC

formation (i.e. cyclogenesis, from A to D) and EC dissolution (i.e. cyclolysis, form D to G). When the balance in Eq. (4) is negative the cyclogenesis occurs so that the critical phase of the EC is in the proximity of point D where negative terms overcome the positive one.

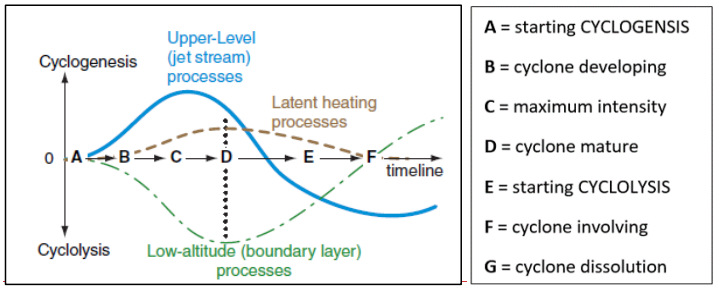

Figure 3: Qualitative temporal evolution of each of four terms T1, T2 and T3 during cyclone phases (A to G) and their contribution to cyclone formation (cyclogenesis) and cyclone dissolution (cyclolysis), proposed in (Stull, 2017), modified after.

3 Results and Discussion

The first approach, based on the definition of critical events against threshold curves, carried out the analysis only on rainfall parameters, i.e. the rain intensity (I) and the duration (D). The second extended the precipitation study considering also other meteorological parameters, reported inside NCEP reanalysis maps, and applying the model proposed in Eq. (4) for EC intensity.

3.1 Approach 1: the Rainfall Analysis

Considering the average daily rain rate I and the duration D of the rainfall episodes reported in Table 1, these data were plotted against the rainfall threshold curves listed from Eq. (2.a) to Eq. (2.e) inside Figure 4. A large number of events can be clustered in the right-bottom corner of the graph due to their characteristics of a rather long duration 2-4 days and slightly low intensities. Only the event of 2019, 2008 and 1953 are dispersed on the other side of the graph where the duration is around or less than a day.

Considering the thresholds proposed by (Guzzetti et al., 2007), all the events points are correctly settled above lines. In particular, no big differences are seen among the general one (3), the curve valid for mid-latitude climate (4) and the one valid for highlands climate (5). On the other hand, the thresholds proposed by Ceriani (2) and Caine (1) are settled above the previous. The "Ceriani" one seems to fit very well the data, posing only the 1966 event slightly below the curve and the 1953 and 1960 close to the curve. This result was expected because the "Ceriani" threshold has been calibrated using a dataset of local events until 1994. Conversely, the "Caine" threshold seems to work worst rather than the previous. 1953,

1960 and the 1966 events are not identified as critical and appear below the curve. In this case, the threshold curve has been unable to detect these events. Moreover, the 1997 and 2000 are settled borderline on the curve.

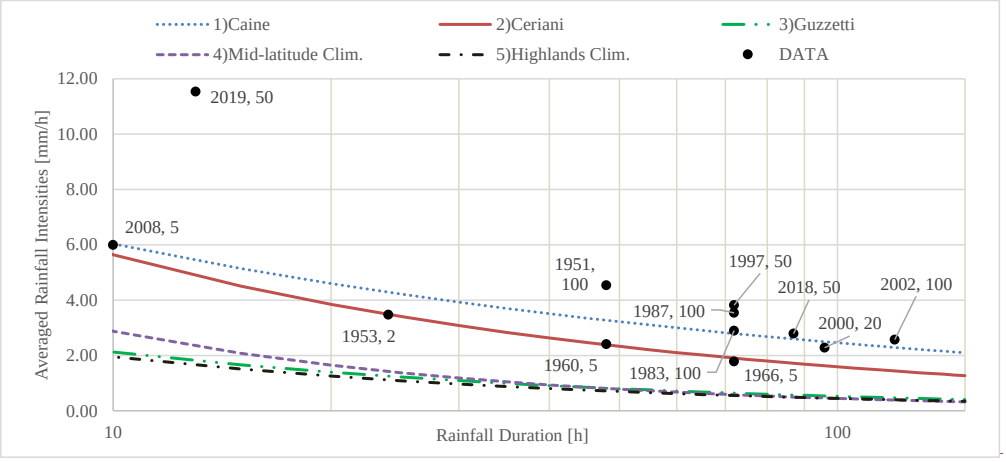

Figure 4: Intensity-Duration relationship for considered events and relative precipitation RP.

For each critical event, the related rainfall return period has been also specified in Figure 4. According to (Gao et al., 2018; Iida, 2004; Rosso et al., 2006), a beam of rainfall intensity-duration curves can be elaborated including their dependence from RP. Considering the "Ceriani" threshold, the critical events that exhibit higher RPs are located at higher distances from the curve and, on the other hand, the events with a small return time are settled nearer. Therefore, the vertical distance between the curve and the critical event point could be addressed as a possible indicator of the magnitude of the hydrogeologicalgeo-hydrological events, but the empirical correlation founded in these literature analyses suggests that it may be subjected to large uncertainties (Gao et al., 2018).

In conclusion, the threshold curves assess if a rainfall event can trigger hydrogeologicalgeo-hydrological issue, but no further detailed information can be retrieved to the effective magnitude of the event occurred. The physical nature description of the rainfall phenomena is generally missed and a relative comparison among the different critical events cannot be properly done. In addition, the wide range of threshold curves available for the area and their empirical evaluation increase the uncertainty around the assessment of the critical events. Moreover, the small database of our study does not permit us to clearly assess a magnitude of the hydrogeologicalgeo-hydrological event simply looking at these distances among the threshold and each critical event point.

A further step of the analysis has been carried out considering not only the information about the intensities of the triggering phenomena but also their spatial extension, i.e. "EXL" or "DIF".

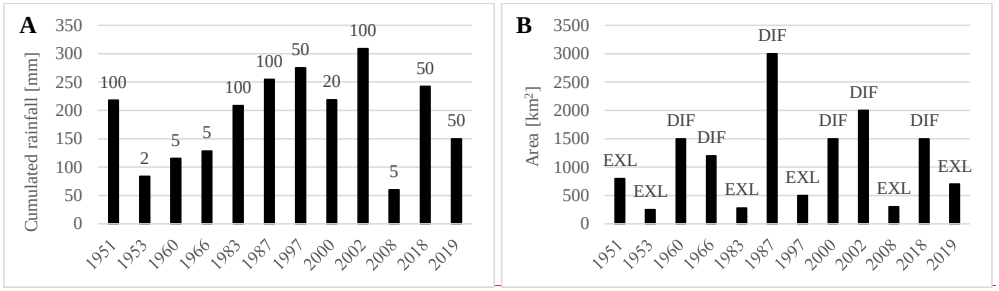

Figure 5: Cumulated rainfall and RP of triggering events (A) and the Area affected by hydrogeologicalgeo-hydrological issues (B).

Looking at Figure 5.A, the Sondrio Province has experienced at least four exceptional rainfall events with a return period equal to 100 years: 1951, 1983, 1987 and 2002. From RP analysis, they were ranked with the same intensity but among them 1987 has been recorded historically as the most catastrophic one, i.e. with the highest magnitude, that affected the area in the second half of the XX century. This apparent contradiction has a possible explanation considering the information about the spatial extension of the affected areas, as reported in Figure 5.B, which is a property strictly related to the nature of the rainfall event (Corominas et al., 2014; Gao et al., 2018). Those were not directly considered in RP evaluation that takes into account only the local amount of precipitation or an averaged value across a region. Therefore, if only the RP is considered, 1983 is intended to be intense as 1987, but, considering the spatial distribution the 1983 event affected only a limited area and the 1987 spread across the entire province. In this light, the RP information leads to a false interpretation of the nature of the two triggering phenomena and it cannot be considered directly for establishing a magnitude of the related hydrogeologicalgeo-hydrological consequences on the territory.

According to (Corominas et al., 2014), the hazard intensity of a hydrogeologicalgeo-hydrological event can be addressed considering three different contributes. Excluding the territorial susceptibility, the extension of the affected area and the intensity of the triggers are the other two main components. In scientific literature, it does not exist a unique method for the magnitude assessment of a hydrogeologicalgeo-hydrological episode because its quantification depends on the type of triggered phenomena involved and on the scope of the hazard study (Corominas et al., 2014; ISPRA, 2018). In the special case of the rainfall-induced shallow landslides, a logarithmic function seems to explain roughly the relationship among the event magnitude and the characteristics of the trigger. According to (Malamud et al., 2004), a magnitude index can be defined as a logarithmic function of the number of triggered landslide and considering the study of (Bovolo and Bathurst, 2011; Frattini et al., 2009; Reid and Page, 2003), a similar frequency-magnitude relation can be found for the intensity of rainfall event. Based on these evidences, two indices m_1 and m_2 have been considered for defining the magnitude of analysed hydrogeologicalgeo-hydrological events, taking into account the fact that both the spatial extension and the intensity of triggering are involved in its definition.

$$m_1 = \log_{10}(Area\ Affected) \quad (5.a)$$

$$m_2 = \log_{10}(Return\ Period) \quad (5.b)$$

These two indexes were calculated and normalized among 0 and 1 for each considered event and then compared. Not surprisingly, looking at Figure 6, they brought complementary information. In the case of 1987 and 2002, both events experienced higher values of the index m_1 and m_2 that are in accordance with the previous observations, i.e. intense event and rather spatial diffuse. On the contrary, 1983 shows a low value of m_1 and high one for m_2, i.e. a very localized event but also particularly intense. In order to give a unique and quantitative ranking of the event's magnitude, for each events the indices m_1 and m_2 have been averaged (AVG). The latter was considered as a reference for the comparison with the SLPT physically based index proposed in the meteorological reanalysis approach.

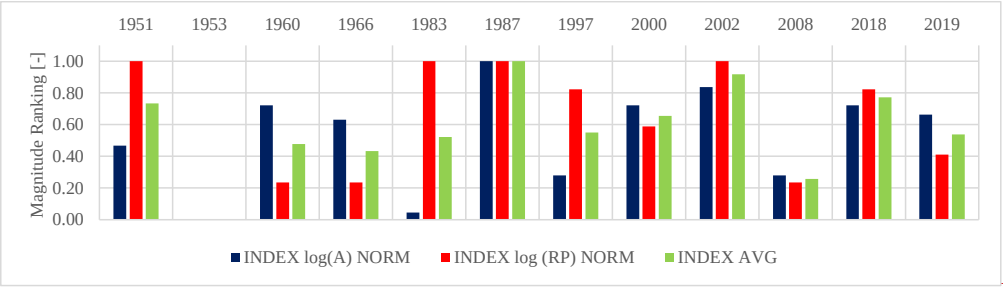

Figure 6: Event magnitude ranking considering the two normalized index "log(A)" and "log(RP)" and their average "AVG".

3.2 Approach 2: Meteorological Analysis

The second approach consists of the application of the model proposed by (Stull, 2017) and described in Eq.(4). Atmospheric pressure gradients, wind velocities, and air masses advection through the Alpine region were studied for feeding each of the model components illustrated in the Equation (4.a), (4.b), and (4.c). According to (Stull, 2017), the sea-level pressure tendency index (SLPT) $\Delta p_s/\Delta t$ [hPa/h] was calculated for assessing the intensity of the meteorological triggering events. This estimation has been done in correspondence to the critical phase of each event, i.e. the "D" phase of the scheme reported in Figure 3.

3.2.1 Wind Components

For determining the $T1$ term ("upper layer divergence" Equation (4.a)), the dynamic of geostrophic wind components was examined considering the NCEP reanalysis maps.

Geostrophic wind is the theoretical wind that would result from an exact balance between the Coriolis force and the pressure gradient force and it is a valuable first approximation of the general circulation of the air masses at a regional scale (Andrews, 2010; Martin, 2006; Stull, 2017). Generally, intense geostrophic wind means that the pressure gradient between a

low and high pressure is sharp, and it is associated with strong EC structures (Figure 2). Therefore, geostrophic wind velocity is an indicator of the meteorological event intensity (Stull, 2017).

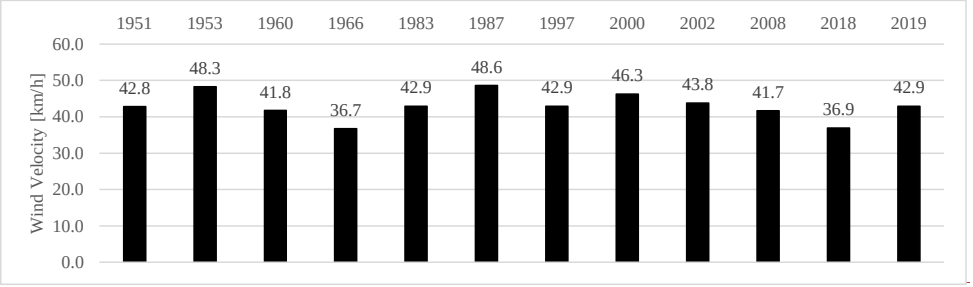

Figure 7: Geostrophic velocity comparisons.

The geostrophic wind velocity, calculated in correspondence of the central phase of the event (stage "D" in Figure 3), exhibit a range comprised between 35 km/h – 50 km/h (Figure 7). The results show that the events characterized by higher velocities have been also interested in more intense rainfall, such as the case of 1987, but on average the events have shown similar values. Regarding the wind direction, not reported, it was observed that all the events have been characterized by the presence of sustained southern flows at 850 hPa geopotential height. This evidence is in accordance with the typical air masses configuration that characterizes this type of event where orographic precipitations are enhanced in intensity and they are generally prolonged for several hours or days (Grazzini, 2007; Rotunno and Houze, 2007). The interpretation of geostrophic balance of wind is generally valid at large scale but it does not take into account the secondary effects that can modify consistently the local intensities of rainfall phenomena (Martin, 2006; Stull, 2017). Therefore, other terms of Eq. (4) are further discussed.

3.2.2 Air Masses Evolution Paths

For determining the $T2$ term, ("boundary layer pumping" Equation (4.b)), the air masses evolution paths were examined during each event. Respect to the $T1$ and $T3$ terms, it acts inhibiting the ECs development and it is rather influenced by ECs latitude evolution. In fact, ECs do not follow the same advection path seasonally and this is a key parameter for distinguishing and interpreting different types of rainfall events.

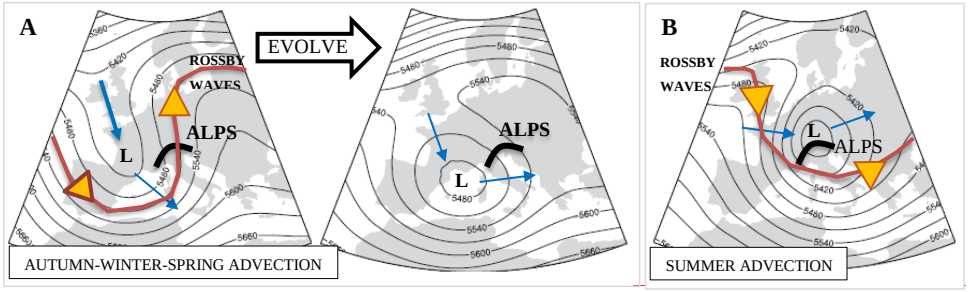

Figure 8: Extratropical Cyclone latitude extensions where are reported the most common air masses configurations for the autumnal and spring (A) and summer events (B), adapted from (Panziera, et al., 2015), modified after.

Looking at Figure 8.A the larger part of the autumnal events exhibits a meridian motion of the low pressure from the northern part of Europe (Northern Sea) to the southern part, entering the Mediterranean Sea and moving eastward following Rossby waves track (Rotunno and Houze, 2007; Stull, 2017). This is the case of 1960, 1966, 2000, 2002 and 2018 events occurred between September and November. Autumnal periods are also characterized by the presence of high-temperature gradient between the Mediterranean Sea (warm) and the North Atlantic region (cold) which leads to the formation of strong EC structures more frequently (Rotunno and Houze, 2007; Stull, 2017).

Summer events of 1951, 1953, 1987, 1997 and 2019 exhibit a low pressure tracking path that did not cross the Alps mountain range (Figure 8.B). This fact can be explained by considering that Rossby waves are in general northern shifted and less meandered during the summer period (Grazzini and Vitart, 2015; Martin, 2006). This reflects on the events that affect the southern side of the alpine region which are more rapid, less persistent, locally intense but not well organized such as the typical autumnal EC. In this framework, 1987 has assumed a character of exceptionality due to its anomaly features regarding, in particular, its temporal persistence on the examined area.

3.2.3 Sea-Level Pressure Tendency Index

The $T3$ term has not explicitly analysed because it is represented as a linear function of the daily rainfall rate RR, which was already considered in the precipitation analysis. In particular, it is an expression of the local effects of the ECs on the territory, i.e. the rainfall intensity, and it is intimately bound with the thermodynamic of the ECs structure (Martin, 2006), acting positively for its development (Stull, 2017).

In the end, the analysis of the intermediate components of the EC model $T1$, $T2$ and $T3$ terms allowed defining the Sea-Level Pressure Tendency index (SLPT) of Eq. (4).

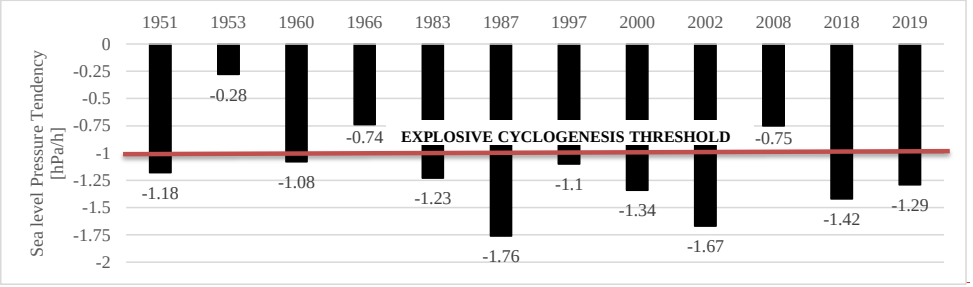

Figure 9: Sea-Level Pressure Tendency Index (SLPT) for the event analysed.

Looking at Figure 9, the SLPT index shows a range comprised between the -0.28 hPa/h, recorded for the 1953 event and -1.76 hPa/h recorded for 1987. The latter and the 2002 (-1.67 hPa/h) are reported to have been the EC structures with the highest intensity that affected the Northern Lombardy area. An important characteristic is that some of these ECs have been characterized by explosive cyclogenesis. Explosive cyclogenesis happens when an extratropical cyclone exhibits in its central part a low pressure deepening of 24 hPa in 24 h, which corresponds to an average rate of 1 hPa/h (Sanders and Gyakum, 1980). They are potentially dangerous for the territory due to their rapid evolution, causing flash floods and diffuse hydrogeologicalgeo-hydrological issues that, in our case, have been confirmed by the historical chronicles found in the AVI and IFFI databases.

3.3 Magnitude Indexes Comparison

The SLPT index has been able to assess through a physical formulation the intensity of the meteorological triggering factors of the hydrogeologicalgeo-hydrological event examined. Considering the rather strong cause-effect relation that was highlighted by historical chronicle among the intensity of the rainfall episodes and the severity of the subsequent hydrogeologicalgeo-hydrological issues, the SLPT index was tested as a predictor of the hazard magnitude. In order to address this, the index was normalized among 0 and 1 and then compared with the empirical index (AVG index) proposed within rainfall analysis, that represent in our study the reference for magnitude evaluation.

Looking at Figure 10 it is rather clear how the two indexes, the empirical and the physical based, are in accordance, giving a similar magnitude ranking of the events studied. In particular, both have addressed again the 1987 and 2002 as the two most critical of the entire dataset and have ranked 1953 as the lowest intense. For the other events, the ranking was rather similar showing an overall root mean square error (RMSE) less than 7%.

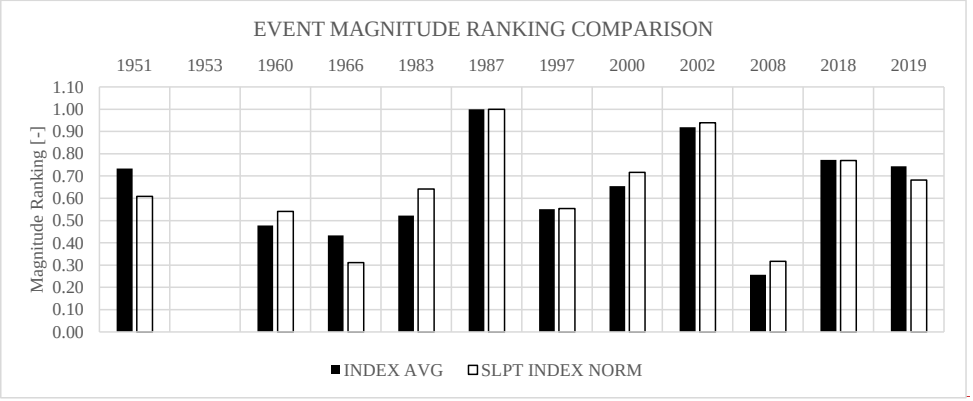

Figure 10: Event magnitude comparison between the SLPT index and the AVG index. The two indexes are normalized among 0 and 1.

The result obtained here are representative of the qualitative information found inside the historical database analysed, where an objective criterion for the magnitude quantification was not applicable due to poorly data reported (ISPRA, 2018). In this light, NCEP reanalysis map have represented an important source for the quantitative interpretation of the meteorological triggering factors in correspondence of the critical events analysed, allowing also a more complete examination of the severity of the subsequent rainfall induced hydrogeologicalgeo-hydrological events.

4 Conclusions

This study presented an extended back analysis of the triggering meteorological factors that have caused in the past several hydrogeologicalgeo-hydrological issues in the alpine mountain territory of the Sondrio Province, Northern Lombardy, Italy. Excluding the analysis of the local geomorphological predisposing causes, the attention was pointed out on the characteristics of rainfall that were considered as the primary cause of hydrogeologicalgeo-hydrological hazards analysed. The main goal of the study was to develop a quantitative analysis of the meteorological triggering factors that were able to explain the magnitude of the rainfall induced hydrogeologicalgeo-hydrological issues that affected the studied area. Two different approaches have been proposed: the first one considered the local information about rainfall amounts, intensities, and durations for characterizing the critical events through the rainfall threshold curves. The second takes into account other meteorological parameters implicated in the physical description of a rainfall phenomenon.

Following the first approach, the rainfall threshold curves have been able to predict the instabilities, but no useful information was gathered for the magnitude assessment of the hydrogeologicalgeo-hydrological events. The analysis was improved considering the return period of precipitation. Nevertheless, looking only at the RPs may lead to a misleading and

wrong interpretation of the triggering causes because recorded rain-gauges data series represent a local estimation of the rainfall event intensity. The RP values do not take into account explicitly the spatial distribution of the meteorological phenomena that are directly correlated to the consequent hydrogeologicalgeo-hydrological issues triggered in the territory. Therefore, a composite magnitude index for assessing a ranking of hydrogeologicalgeo-hydrological events considered has been proposed taking into account not only the intensity of the triggers, i.e. return period of rainfalls, established from the analysis of the rainfall series, but also the information about the spatial extension of the affected areas.

In the second approach, a meteorological analysis of the triggering has been carried out taking into account the NCEP reanalysis maps. The model in Eq. (4) was implemented for the description of each meteorological event intensities through the physically based index SLPT. This index was chosen because considers not only the local rain-gauges series but also other meteorological variables that are descriptive of the whole dynamic of the triggering event. That physical index was then normalized and compared with the previous empirical one obtained from the analysis of precipitation data.

Both two indices have shown good accordance in the assessment of the magnitude of the studied events. In particular, the 1987 and the 2002 events have been correctly ranked as the strongest of the entire dataset, caused by explosive cyclogenesis. Respect to the m_1 and m_2 indices that are based on empirical evidence extracted from local data analysis, the SLPT indicator is physically based and can discriminate straightforwardly localized events "EXL" with respect to the more diffused ones "DIF", that is a key information. The hydrogeologicalgeo-hydrological issues that affected the alpine territory were proportional to the overall intensity of extratropical cyclone systems and the SLPT index has been able to highlight this fact, also distinguishing the nature of the triggers.

In the view of the future climate change that, with high confidence (Faggian, 2015), will affect the Mediterranean and the Alpine environment, extreme meteorological events are supposed to increase (Ciervo et al., 2017; Gariano and Guzzetti, 2016; Moreiras et al., 2018). Our study moves in this direction, trying to consider integration between the traditional approach (i.e. local rainfall analysis) and the new instruments that meteorological models are starting to provide (i.e. meteorological reanalysis map) in order to give a comprehensive interpretation of the triggering factors of severe hydrogeologicalgeo-hydrological events.

Code and data availability: All the data reported in this paper are freely consultable on the Internet websites. In particular, reanalysis weather maps are freely downloadable from Meteociel Website (MeteoCiel, 2020), IFFI and AVI database are freely consultable and downloadable from (CNR, 2020; ISPRA, 2014), and Rain Gauges data are extracted from local Environmental Agency (ARPA Lombardia, 2020). The model applied in this work is also freely consultable and downloadable from (Stull, 2017).

Author Contribution: Andrea Abbate carried out the formal analysis and prepared the manuscript with contributions from all co-authors. Monica Papini supervised the research and Laura Longoni the review & editing.

Competing Interests: The authors declare that they have no conflict of interest.

References

Abbate, A., Longoni, L., Ivanov, V. I. and Papini, M.: Wildfire impacts on slope stability triggering in mountain areas, MDPI Geosciences, 9(417), 1–15, doi:https://doi.org/10.3390/geosciences9100417, 2019.

Albano, R., Mancusi, L. and Abbate, A.: Improving flood rick analysis for effectively supporting the implementation of flood risk management plans: The case study of "Serio" Valley, Envirnomental Science & Policy, 75, 158–172, doi:https://doi.org/10.1016/j.envsci.2017.05.017, 2017.

Andrews, D. G.: An Introduction to Atmospheric Physics, Cambridge Press, Cambridge., 2010.

ARPA Lombardia: Rete Monitoraggio Idro-nivo-meteorologico, [online] Available from: www.arpalombardia.it/stiti/arpalombardia/meteo, 2020.

Ballio, F., Brambilla, D., Giorgetti, E., Longoni, L., Papini, M. and Radice, A.: Evaluation of sediment yield from valley slope, Transactions on Engineering Sciences, 67, 149–160, doi:http://doi.org/10.2495/DEB100131, 2010.

Bovolo, C. I. and Bathurst, J. C.: Modelling catchment-scale shallow landslide occurrence and sediment yield as a function of rainfall return period, Hydrological Processes, 26, 579–596, doi:https://doi.org/10.1002/hyp.8158, 2011.

Caine, N.: The rainfall intensity duration control of shallow landslide and debris flow, Geografisika Annaler, 62(1–2), 659–675, doi:https//doi.org/10.2307/520449, 1980.

Ceriani, M., Lauzi, S. and Padovan, M.: Rainfall thresholds triggering debris-flow in the alpine area of Lombardia Region, central Alps – Italy, in In Proceedings of the Man and Mountain'94, Ponte di Legno (BS), Italy., 1994.

Ciccarese, G., Mulas, M., Alberoni, P., Truffelli, G. and Corsini, A.: Debris flows rainfall thresholds in the Apennines of Emilia-Romagna (Italy) derived by the analysis of recent severe rainstorms events and regional meteorological data, Geomorphology, 358, 1–20, doi:https://doi.org/10.1016/j.geomorph.2020.107097, 2020.

Ciervo, F., Rianna, G., Mercogliano, P. and Papa, M. N.: Effects of climate change on shallow landslides in a small coastal catchment in southern Italy, Landslide, 14, 1043–1055, doi:https://doi.org/10.1007/s10346-016-0743-1, 2017.

CNR: Sistema Informativo sulle Catastrofi idrogeologiche, [online] Available from: www.db.gndci.cnr.it, 2020.

COPERNICUS: Monitoring European climate using surface observations, [online] Available from: http://surfobs.climate.copernicus.eu/surfobs.php, 2020.

Corominas, J., van Westen, C., Frattini, P., Cascini, L., Malet, J.-P., Fotopoulou, S., Catani, F., Van Den Eeckhaut, M., Mavrouli, O., Agliardi, F., Pitilakis, K., Winter, M. G., Pastor, M., Ferlisi, S., Tofani, V., Hervás, J. and Smith, J. T.: Recommendations for the quantitative analysis of landslide risk, Bulletin of Engineering Geology and the Environment, 73(2), 209–263, doi:10.1007/s10064-013-0538-8, 2014.

De Michele, C., Rosso, R. and Rulli, M. C.: Il Regime delle Precipitazioni Intense sul Territorio della Lombardia: Modello di Previsione Statistica delle Precipitazioni di Forte Intensità e Breve Durata, ARPA Lombardia, Milano., 2005.

Faggian, P.: Climate change projection for Mediterranean Region with focus over Alpine region and Italy, JESE, 4, 482–500, doi:https://dori.org/10.17265/2162-5263/2015.09.004, 2015.

Frattini, P., Crosta, G. and Sosio, R.: Approaches for defining thresholds and return periods for rainfall-triggered shallow landslides, Hydrological Processes, 23(10), 1444–1460, doi:10.1002/hyp.7269, 2009.

Gao, L., Zhang, L. M. and Cheung, R. W. M.: Relationships between natural terrain landslide magnitudes and triggering rainfall based on a large landslide inventory in Hong Kong, Landslides, 15(4), 727–740, doi:10.1007/s10346-017-0904-x, 2018.

Gariano, S. L. and Guzzetti, F.: Landslides in a changing climate, Earth-Science Reviews, 162, 227–252, doi:10.1016/j.earscirev.2016.08.011, 2016.

Godson, W. L.: A new tendency equation and its application to the analysis of surface pressure changes, Journal of Meteorology, 5, 227–235, 1948.

Grazzini, F.: Predictability of a large-scale flow conducive to extreme precipitation over the western Alps, Meteorology and Atmospheric Physics, 95(3), 123–138, doi:10.1007/s00703-006-0205-8, 2007.

Grazzini, F. and Vitart, F.: Atmospheric predictability and Rossby wave packets, Quarterly Journal of the Royal Meteorological Society, 141(692), 2793–2802, doi:10.1002/qj.2564, 2015.

Guzzetti, F., Peruccacci, S., Rossi, M. and Stark, C. P.: Rainfall thresholds for the initiation of landslides in central and southern Europe, Meteorology and Atmospheric Physics, 98(3), 239–267, doi:10.1007/s00703-007-0262-7, 2007.

Iida, T.: Theoretical research on the relationship between return period of rainfall and shallow landslides, Hydrological Processes, 18(4), 739–756, doi:10.1002/hyp.1264, 2004.

ISPRA: Inventario Fenomeni Franosi, [online] Available from: http://www.isprambiente.gov.it/it/progetti/suolo-e-territorio-1/iffi-inventario-dei-fenomeni-franosi-in-italia, 2014.

ISPRA: Dissesto idrogeologico in Italia: pericolosità e indicatori di rischio, ISPRA, Ispra., 2018.

ISPRA: SCIA: Sistema Nazionale per l'elaborazione e diffusione di dati climatici, [online] Available from: http://www.scia.isprambiente.it, 2019.

Iverson, R. M.: Landslide triggering by rain infiltration, Water Resources Research, 36(7), 1897–1910, doi:10.1029/2000WR900090, 2000.

Kalnay, E., Kanamitsu, M., Kistler, R., Collins, W., Deaven, D., Gandin, L., Iredell, M., Saha, S., White, G., Woollen, J., Zhu, Y., Chelliah, M., Ebisuzaki, W., Higgins, W., Janowiak, J., Mo, K. C., Ropelewski, C., Wang, J., Leetmaa, A., Reynolds, R., Jenne, R. and Joseph, D.: The NCEP/NCAR 40-Year Reanalysis Project, Bull. Amer. Meteor. Soc., 77(3), 437–472, doi:10.1175/1520-0477(1996)077<0437:TNYRP>2.0.CO;2, 1996.

Longoni, L., Papini, M., Arosio, D. and Zanzi, L.: On the definition of rainfall thresholds for diffuse landslides, Transactions on State of the Art in Science and Engineerin, 53(1), 27–41, doi:https://doi.org/10.2495/978-1-84564-650-9/03, 2011.

Longoni, L., Ivanov, V. I., Brambilla, D., Radice, A. and Papini, M.: Analysis of the temporal and spatial scales of soil erosion and transport in a Mountain Basin, Italian Journal of Engineering Geology and Environment, 16(2), 17–30, doi:https://doi.org/10.4408/IJEGE.2016-02.O-02, 2016.

Malamud, B. D., Turcotte, D. L., Guzzetti, F. and Reichenbach, P.: Landslide inventories and their statistical properties, Earth Surface Processes and Landforms, 29(6), 687–711, doi:10.1002/esp.1064, 2004.

Martin, J. E.: Mid-Latitude Atmosphere Dynamics, Wiley, Chichester, West Sussex, England., 2006.

MeteoCiel: Observations, Prévisions, Modèles en temps réel, [online] Available from: www.meteociel.fr, 2020.

Montrasio, L.: Stability of soil-slip, Wit Press, Risk Analysis II, 45, 357–366, doi:https://doi.org/10.2495/RISK000331, 2000.

Montrasio, L. and Valentino, R.: Modelling Rainfall-induced Shallow Landslides at Different Scales Using SLIP – Part II, Procedia Engineering, 158, 482–486, doi:10.1016/j.proeng.2016.08.476, 2016.

Moreiras, S., Vergara Dal Pont, I. and Araneo, D.: Were merely storm-landslides driven by the 2015-2016 Niño in the Mendoza River valley?, Landslides, 15, doi:10.1007/s10346-018-0959-3, 2018.

NOAA: National Center for Environmental Information, [online] Available from: https://www.ncei.noaa.gov/, 2020.

Olivares, L., Damiano, E., Mercogliano, P., Picarelli, L., Netti, N., Schiano, P., Savastano, V., Cotroneo, F. and Manzi, M. P.: A simulation chain for early prediction of rainfall-induced landslides, Landslides, 11(5), 765–777, doi:10.1007/s10346-013-0430-4, 2014.

Ozturk, U., Tarakegn, Y., Longoni, L., Brambilla, D., Papini, M. and Jensen, J.: A simplified early-warning system for imminent landslide prediction based on failure index fragility curves developed through numerical analysis, Geomatics, Natural Hazards and Risk, doi:10.1080/19475705.2015.1058863, 2015.

Papini, M., Ivanov, V., Brambilla, D., Arosio, D. and Longoni, L.: Monitoring bedload sediment transport in a pre-Alpine river: An experimental method, Rendiconti Online della Società Geologica Italiana, 43, 57–63, doi:10.3301/ROL.2017.35, 2017.

Peres, D. J., Cancelliere, A., Greco, R. and Bogaard, T. A.: Influence of uncertain identification of triggering rainfall on the assessment of landslide early warning thresholds, Natural Hazards and Earth System Sciences, 18(2), 633–646, doi:10.5194/nhess-18-633-2018, 2018.

Piciullo, L., Gariano, S. L., Melillo, M., Brunetti, M. T., Peruccacci, S., Guzzetti, F. and Calvello, M.: Definition and performance of a threshold-based regional early warning model for rainfall-induced landslides, Landslides, 14(3), 995–1008, doi:10.1007/s10346-016-0750-2, 2017.

Rappelli, F.: Definizione delle soglie pluviometriche d'innesco frane superficiali e colate torrentizie: accorpamento per aree omogenee, IRER, Istituto Regionale di Ricerca della Lombardia, Milano., 2008.

Reid, L. and Page, M. J.: Magnitude and frequency of landsliding in a large New Zealand catchment, Geomorphology, 49, 71–88, doi:10.1016/S0169-555X(02)00164-2, 2003.

Rosi, A., Peternel, T., Jemec-Auflič, M., Komac, M., Segoni, S. and Casagli, N.: Rainfall thresholds for rainfall-induced landslides in Slovenia, Landslides, 13(6), 1571–1577, doi:10.1007/s10346-016-0733-3, 2016.

Rossi, M., Guzzetti, F., Salvati, P., Donnini, M., Napolitano, E. and Bianchi, C.: A predictive model of societal landslide risk in Italy, Earth-Science Reviews, 196, 102849, doi:10.1016/j.earscirev.2019.04.021, 2019.

Rosso, R., Rulli, M. C. and Vannucchi, G.: A physically based model for the hydrologic control on shallow landsliding, Water Resour. Res, 42, doi:10.1029/2005WR004369, 2006.

Rotunno, R. and Houze, R.: Lessons on orographic precipitation for the Mesoscale Alpine Programme, Quarterly Journal of the Royal Meteorological Society, 133, 811–830, doi:10.1002/qj.67, 2007.

Sanders, F. and Gyakum, J. R.: Synoptic-Dynamic Climatology of the "Bomb," Mon. Wea. Rev., 108(10), 1589–1606, doi:10.1175/1520-0493(1980)108<1589:SDCOT>2.0.CO;2, 1980.

Stull, R. B.: Practical Meteorology: An Algebra-based Survey of Atmospheric Science., University of British Columbia, Vancouver, Canada., 2017.

Tropeano, D.: Inondazioni e frane in Lombardia: un problema storico, in Utilizzo dei dati storici per la determinazione delle aree esondabili nelle zone alpine, pp. 47–109, CNR-IRPI, Torino., 1997.

Wallace, J. M. and Hobbs, P. V.: Atmospheric Science: an introductory survey, Elsevier, Oxford., 2006.